Large-Volume Microfluidic Cell Sorting for Biomedical Applications

Majid Ebrahimi Warkiani,[1,2] Lidan Wu,[3] Andy Kah Ping Tay,[1] and Jongyoon Han[1,3,4]

[1]BioSystems and Micromechanics IRG, Singapore–MIT Alliance for Research and Technology (SMART) Centre, Singapore 138602; email: jyhan@mit.edu

[2]School of Mechanical and Manufacturing Engineering, Australian Centre for NanoMedicine, University of New South Wales, Sydney, New South Wales 2052, Australia

[3]Department of Biological Engineering and [4]Department of Electrical Engineering and Computer Science, Massachusetts Institute of Technology, Cambridge, Massachusetts 02139

Annu. Rev. Biomed. Eng. 2015. 17:1–34

First published online as a Review in Advance on July 16, 2015

The *Annual Review of Biomedical Engineering* is online at bioeng.annualreviews.org

This article's doi: 10.1146/annurev-bioeng-071114-040818

Keywords

cell sorting, high-throughput, large-volume microfluidic, circulating cancer cells, blood transfusion, inertial, sepsis, separation

Abstract

Microfluidic cell-separation technologies have been studied for almost two decades, but the limited throughput has restricted their impact and range of application. Recent advances in microfluidics enable high-throughput cell sorting and separation, and this has led to various novel diagnostic and therapeutic applications that previously had been impossible to implement using microfluidics technologies. In this review, we focus on recent progress made in engineering large-volume microfluidic cell-sorting methods and the new applications enabled by them.

Contents

1. INTRODUCTION

The advent of microfabrication, precision engineering, and rapid prototyping techniques has accelerated the growth of microfluidic technology since the early 1990s, making it an ideal platform to bridge the gap between wet sciences (biology and chemistry) and engineering (1). The scale of microfluidic systems and their resemblance to 3D physiological environments provide a compatible interface for manipulating cells and imitating in vivo conditions. The ability to sort cells enables important discoveries in cell biology, thus further enabling diverse biomedical applications in a variety of areas including HIV diagnostics (2) and cancer therapy (3).

Historically, microfluidics evolved out of microscale capillary electrophoresis (4), the main selling points of which were fast and efficient sample processing (that is, separation) and the requirement for only small samples. Although these are highly attractive and novel features for analytical chemistry, they also represent a significant limitation of microfluidics technology because they lead to low throughput and give rise to issues of world-to-chip interfacing.

The typical sample volumes used in microfluidics (up to approximately 1 nL) and the flow rates achievable in microfluidic systems (up to approximately 1 μL/min) are incompatible with the typical biosample volumes used in biochemistry and clinical diagnostics (usually ranging from 1 μL to approximately 1 mL). These limitations are especially detrimental for detecting and recovering low-abundance targets, such as low-abundance circulating tumor cells (CTCs) and blood-borne pathogens, whose clinically relevant abundance ranges approximately from 1 to 100 cells/mL. Often, the scarcity of these targets requires processing at least 1–10 mL of raw blood just to collect sufficient targets for meaningful and reliable downstream analysis. In addition, applications that have been proposed for microfluidic implementation, such as blood dialysis [e.g., an artificial kidney (5)], may require macroscopic-volume flow rates of up to a few liters per minute.

Within the past 5 years, new ideas in microfluidics (such as inertial microfluidics platforms) have enabled cell sorting and separation using much larger volumes and much higher flow rates, leading to various novel diagnostic and therapeutic applications that previously had been deemed impossible. With the new large-volume microfluidics technologies, one can now consider bringing innovations to many important areas, such as filtration. These applications are different from the original vision of microfluidics that emphasized the vertical integration of components, from sample intake to readout. Rather, microfluidics can now be considered a drop-in replacement that has much more functionality and specificity, which is enabled by microfluidic control of cells and targets, but still provides macroscopic flow rates and volumes.

Many good reviews have already been published on the subject of cell separation and microfluidic cell-sorting techniques (6–11). In this review, we focus only on the microfluidic technologies that are enabling these new high-volume applications (i.e., systems that can generate throughput of milliliters per minute). **Table 1** illustrates the various separation methods reviewed in this paper. In addition, we also provide case studies of current and emerging examples of large-volume microfluidic cell-sorting applications, the list of which will lengthen in the coming years.

2. HIGH-VOLUME CELL-SORTING TECHNOLOGIES

2.1. Microfluidic Microfiltration

The age-old method for separating particles is to use physical barriers, and this technique is widely used in many large-volume applications. Filtration processes can be incorporated into microfluidic platforms, and offer many added benefits, including precise control of pore size, filter orientation, and geometry, and more control of the interaction between the filter structure and filtrates (12, 13). In the context of microfluidics, three major designs have been employed for cell-separation purposes, namely weir, pillar, and crossflow (**Figure 1*a***). The weir-type design includes an array of individual barriers that obstruct the flow path to trap cells of a certain size while allowing smaller constituents to pass through narrow slits located on top of the barrier. In other designs, this barrier can be altered by using an array of well-ordered micropillars with different shapes [e.g., crescent-shaped isolation wells (14)] where the main flow is either perpendicular or tangential to the filters. The first use of micromachined silicon filters for blood fractionation was introduced by Wilding and colleagues (15). They designed a weir-type filter with a 3.5 μm gap between the silicon structures and the top layer to effectively isolate white blood cells (WBCs) from red blood cells (RBCs).

In a recent study, Chung et al. (16) developed a novel, microfluidic cell sorter for isolating and characterizing CTCs from whole blood. Their platform utilized a modified weir-type structure along with fluidic channels (**Figure 1*b***) to continuously separate and capture CTCs at flow rates of up to 20 mL/h. Micropillar arrays with different gap sizes have also been employed to demonstrate the effective isolation of CTCs from blood (26), the enrichment of fetal nucleated red blood cells (27), leukapheresis (28), and the removal of pathogens (29), but their reported throughputs were lower.

One of the inherent problems in both conventional filtration and its microfluidic counterpart is blockage and clogging (i.e., cell buildup over time), leading to shorter operational times and lower throughput (30). In conventional filtration, crossflow filtration is often adopted to mitigate this challenge. Microfluidics offers the additional flexibility of both observing and manipulating filtrate–filter interactions, enabling the design of more intelligent filter structures. For example, Sethu and coworkers (28) showed that leukocyte depletion from whole blood (i.e., apheresis) was

Table 1 High-throughput separation methods reviewed in this article[a]

Method of separation	Mode of separation	Separation criteria	Target sample to be removed	Throughput[b]	Separation efficiency (%)	Remarks	Reference
Microfilter	Size exclusion	Size and deformability	Cancer cells	20 mL/h (0.33 mL/min)	>95	Tested with murine blood; prone to clogging	16
Deterministic lateral displacement	Migration between microposts in an array	Size	Cancer cells	10 mL/min	85	Blood dilution required; prone to clogging	17
Hydrodynamic	Streamline manipulation	Size, shape, and deformability	Droplet separation	160 particles/s[c]	79.2	99% purity with >10,000-fold enrichment	18
Inertial (straight channel)	Lift forces	Size and deformability	Bacteria in 0.5% v/v blood	8 mL/min	80	10% contamination with RBCs (in parallelized version); prone to clogging	19
Inertial (curvilinear channel)	Balance of lift and Dean forces	Size and deformability	Cancer cells	1 mL/min	85	Lysed blood used; can reach >100 mL/min using multiplexing	20
Centrifugal (hydrocyclone with CCE and disk microfluidics)	Ratio of centripetal forces to fluid resistance	Size, density	Particles suspended in fluid	~1–10,000 mL/min	~90	Throughput varies with inlet velocity and particle size; readers are advised to refer to the original paper for more details	21
Affinity (magnetophoresis)	Differential affinity	Surface markers	Cancer cells	10 mL/h (0.17 mL/min)	90	Costly; nonspecific binding	22
Acoustic	Acoustic radiation forces	Size, density, and compressibility	RBCs from whole blood	0.3 mL/min	70	20% of lipid particles remained	23
Biomimetic	Mimicking microvasculature	Size and deformability	Infected RBCs from whole blood	5 μL/min (0.005 mL/min)	~90	Leukocyte contamination; can reach throughput of milliliters per minute using parallelization	24
Integrative	Combination of various techniques	Size, deformability, surface markers, etc.	Cancer cells	8 mL/h (0.13 mL/min)	97	Complicated; difficult to automate	25

Abbreviations: CCE, counterflow centrifugal elutriation; RBC, red blood cell; v/v, volume/volume.

[a]The metrics listed in the table are not representative of all microfluidic particle-sorting techniques; they are examples selected to illustrate the range of particles that can be sorted using these techniques. The numbers in the table are the authors' interpretation of the information provided in the papers cited; readers are encouraged to refer to the original papers for more information.

[b]When throughput values were provided in units other than mL/min in the original paper, the original units are given and the conversion to mL/min is shown in parentheses.

[c]The units for throughput in the original paper were given as approximately 3–7 μL/h for 10× diluted blood. Given that the original work relied on encapsulating cells in droplets before sorting, only the original units for throughput are shown here.

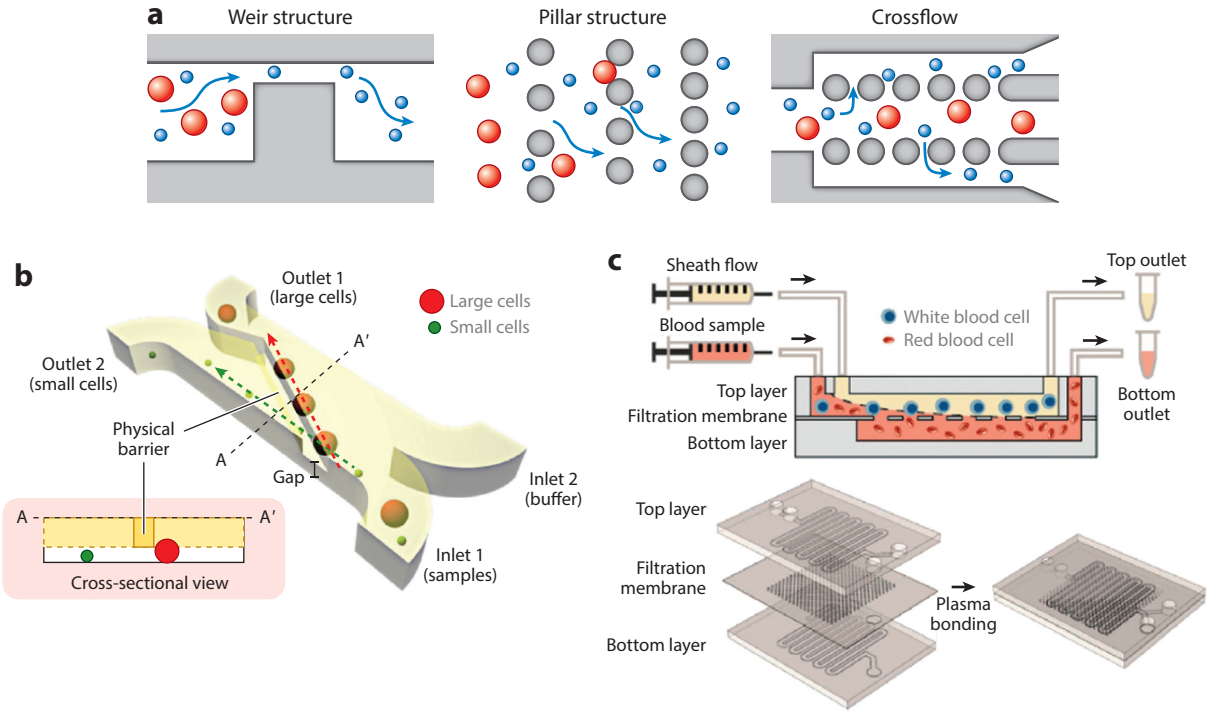

Figure 1

(*a*) Schematic illustrating various microfilter designs. (*Left*) The weir structure excludes cellular components based on their size, allowing smaller cells to pass through a narrow slit. (*Center*) Arrays of pillars with defined pitch that exclude cells larger than the spacing of the pillars. (*Right*) A crossflow microfilter allows continuous separation and collection of both large and small cells from different outlets. (*b*) Schematic illustration of a crossflow microfluidic cell sorter used to separate circulating tumor cells from normal blood cells. Large cancer cells move along the weir-type barrier and are collected at one outlet while smaller hematological cells pass through a gap underneath the barrier, and are directed to a separate outlet. Panel *b* adapted from Reference 16 with permission from Wiley. (*c*) Schematic showing a crossflow microfluidic system with an integrated isopore micromachined filter [made from polydimethylsiloxane (PDMS)] to continuously separate white blood cells from red blood cells in diluted blood samples. Panel *c* adapted from Reference 32 with permission from the Royal Society of Chemistry.

possible without channel clogging, offering the possibility that leukocyte-depleted blood could be returned to the donor. Their device employed microsieves with 2.5 μm gaps that exploited differences in the size and deformability of cells in order to separate them, permitting erythrocytes to pass into side channels while acting as barriers to leukocyte migration. Using the same approach, the same group demonstrated the feasibility of size-based separation of myocytes and nonmyocytes from neonatal rat myocardium in a high-throughput manner (28).

The integration of isoporous microengineered membranes into microfluidic devices has grown substantially during the past 10 years. For example, Aran et al. (31) recently reported integrating polycarbonate track-etched membranes into microfluidic channels to make a crossflow filtration system to continuously extract bacteria from whole blood for the treatment of sepsis. Using membranes with 2 μm pores, they successfully separated smaller bacteria from larger blood cells at a flow rate of approximately 50 μL/min. Instead of integrating a polycarbonate membrane, Li and colleagues (32) designed a simplified approach using surface micromachined polydimethylsiloxane (PDMS) filters inside a microfluidic chip to continuously isolate and sort WBCs from whole

blood, with a sample throughput of 1 mL/h (**Figure 1*c***). Using the same filters, this group has also reported high-throughput (>5 mL/min) isolation and characterization of immune cells that bind to antibody-conjugated polystyrene microbeads (33).

The potential challenges of microfluidic filtration, in addition to clogging and fouling, may include high shear stress on cells trapped during filtration, and poor recovery of captured cells for subsequent characterizations due to the nonspecific adhesion of captured cells (34).

2.2. Hydrodynamic Sorting Techniques

Hydrodynamic-based separation methods constitute the largest portion of microfluidic cell-sorting approaches. Hydrodynamic cell-sorting techniques are passive approaches and rely on no external field or force other than the forces generated by the flow of fluid. Thus, these techniques allow not only easy integration of cell-sorting modules into complex micro total-analysis systems, but also offer the potential for high-throughput cell sorting via device parallelization. Moreover, hydrodynamic approaches are label-free techniques that separate cells based on their physical properties (e.g., size and deformability), and thus avoid the potential interference of biochemical labeling on downstream applications of isolated viable cells. In this section, we review the major hydrodynamic sorting techniques and discuss their application in high-volume sample processing.

2.2.1. Deterministic lateral displacement (operation at low Reynolds numbers). Deterministic lateral displacement (DLD) separates particles by exploiting size-dependent hydrodynamic forces. In DLD, a cell mixture normally passes through a periodic array of micropillars that have a fixed lateral shift between adjacent rows (35). In such platforms, the displacement of the particles is perpendicular to the direction of flow, and particles of different sizes are displaced at different speeds and migration angles. Cells that are smaller than a certain critical hydrodynamic diameter follow the streamlines and pass the micropillars in a cyclically zigzag motion without significant lateral deviation. However, cells that have a diameter larger than the critical threshold cannot completely fit within the streamline and bump against the shifted downstream micropillars into the adjacent streamlines, resulting in accumulative lateral displacement from the small cells (36). Thus, different-sized cells collect at different outlets across the DLD array, leading to continuous separation of the initial sample based on cell size; this method is able to discriminate among cell sizes with very good resolution (i.e., at less than 1% of cell diameter or on the order of 10 nm) (35). Additionally, because the critical diameter of cell separation using DLD is determined by the pattern of the micropillar array, simultaneous separation of subpopulations of cells with distinct diameters could also be achieved by arranging several DLD arrays with different critical thresholds in series within the same chip.

Huang et al. (35) made use of DLD to characterize the separation of beads of different sizes (0.8, 0.9, and 1.0 μm). They were also one of the first groups to apply this concept to isolate artificial bacterial chromosomes. Davis and coworkers (37) reported fractionating blood components (platelets, RBCs, and WBCs) using the DLD technique. Inglis et al. (38) have also applied DLD to purify fungal *Aspergillus* spores of about 4 μm with a density of up to 4.4×10^6 spores/mL. Their device successfully isolated 99% of the target particles while eliminating 96% of smaller and larger particles.

DLD is not limited to sorting relatively smaller particles, such as bacteria and spores; it has also been applied to sorting mammalian cells. Huang et al. (39) used DLD to isolate nucleated RBCs from maternal blood. This technique removed up to 99.99% of RBCs and 99.90% of WBCs. Nonetheless, the flow rate was still low, and blood dilution was necessary. Inglis and coworkers

(40) also captured 98% of WBCs from whole blood with a high throughput of 1 mL/min using parallelized DLD. Davis et al. (37) and Li et al. (41) have also used DLD for the same purpose.

Despite working with relatively small Reynolds numbers (approximately 10^{-1}–10^{-3}), DLD can perform cell separation in a high-throughput fashion when the design is optimal. Based on the separation principle, several factors are known to determine the critical threshold for a particular DLD array, including pillar size, the arrangement of individual micropillars in terms of lateral-position offset, the gap between the pillars, and the angle between the axis of the pillar array and the flow direction (42). Additionally, researchers have identified two other factors that could improve the separation characteristics of DLD systems. One involves careful modification of the channel boundary at each row [based on Inglis's wall design (43)] to eliminate aberrant fluidic flow that may compromise the separation in these regions. The other relies on the shape of the micropillars: recent studies have shown that triangular microposts have superior performance when compared with conventional circular ones, and that triangular microposts result in reduced clogging and fluidic resistance (44). By taking into consideration these two factors, Loutherback et al. (45) recently developed a DLD device (**Figure 2*a***) that can isolate viable CTCs spiked in blood (10^6/mL of CTCs in 10 × diluted blood) with more than 85% recovery and at a relatively high flow rate (10 mL/min). One major limitation of the DLD technique is the sample dilution that results from the introduction of sheath flow during operation; thus, downstream reenrichment of isolated cells might be necessary when dealing with rare cells or when the technique is used in dialysis-like therapy. Some groups have also reported that clogging tended to occur in their devices due to the small critical size and the close proximity of the microposts.

2.2.2. Field-flow fractionation and hydrodynamic filtration (operation at low Reynolds numbers). Hydrodynamic particle-focusing techniques make use of fluid streams with a low Reynolds number to achieve their isolation objectives. In these systems, size-based separation can be achieved by controlling the flow rate, channel geometry, and configuration of outlets (46). Yamada et al. (47) introduced the concept of pinched-flow fractionation to separate polymer microspheres by exploiting their size differences. The ratio of the flow rate of the inlet branches (one with and one without particles) was optimized for efficient sorting; and branches were created at the outlets for collecting the particles independently. Takagi and coworkers (48) used the same concept with asymmetrically branched outlets to isolate RBCs from 0.3% diluted blood. In the study by Takagi and coworkers (48), approximately 80% of the RBCs were enriched in one of the outlets but there were also outlets that had no RBCs. Next, Yamada & Seki (49) introduced hydrodynamic filtration into their device; this consisted of placing multiple branches perpendicular to the inlet (**Figure 2*b***). A small volume of fluid was removed slowly from the main channel via each branch, and the relative fluid-suction rate of the subsequent branch was increased. This process caused smaller particles to be isolated earlier in the device, and larger particles were removed later. WBCs were then enriched using this system and because a smaller volume of fluid was left, the enrichment ratio also increased. Using the same idea, this group also demonstrated high-throughput separation of liver cells (2×10^5 cells/min) (50). In a similar study, Kersaudy-Kerhoas and colleagues (51) created vacuums at multiple branches to influence particle sorting. This technique has also been used to collect blood plasma. Using this technique, it was found that isolation efficiency depended on the ratio of the width of each microchannel to the particle's size. The plasma yield of 40% was superior to other techniques but the purity of the samples was inadequate. Generally, the working flow rates of hydrodynamic techniques are quite low due to the mechanisms used for separation. However, due to the passive nature of this technique parallelization of microfluidic channels is possible, and this can enable high-throughput separation. Moreover, because the mechanism of separation primarily relies on the flow profile

but not directly on the dimensions of the channel, the throughput can be easily increased by using larger channels, which would also minimize clogging.

2.2.3. Inertial separation (operation at moderate Reynolds numbers). In recent years, there has been considerable interest in using inertial microfluidics—which capitalizes on the use of size-dependent hydrodynamic forces in microfluidic channels—in diagnostic, therapeutic, and cell biology applications. As a label-free technique, it manipulates cells and particles in confined microchannels without an externally applied field, and combines the benefits of a passive approach with extremely high throughput and yield (52). Due to the inertial lift forces (i.e., shear-induced lift forces and wall-induced lift forces) arising from the parabolic nature of the laminar velocity profile, randomly dispersed particles or cells migrate across the streamlines to an equilibrium position away from the center of the channel (53). Focusing normally occurs for particles satisfying the confinement ratio $\lambda = a_p/D_h \geq 0.07$, where a_p is the particle diameter and D_h is the hydraulic

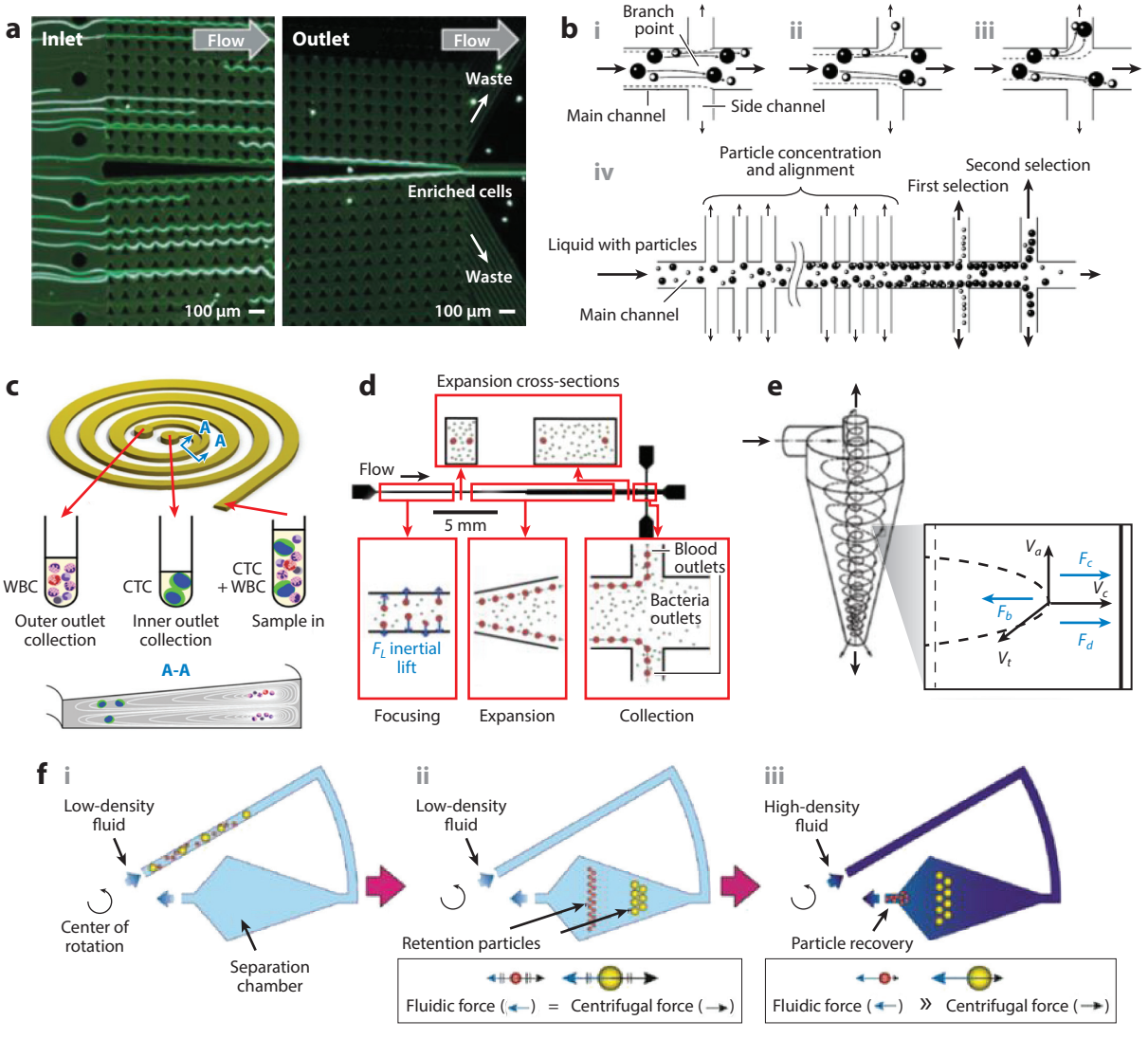

diameter (46). Apart from this, adding curvature to the channel (such as a spiral or serpentine curve) introduces a transverse secondary flow (i.e., a Dean flow). The Dean flow is composed of two counter-rotating vortices (Dean vortices) that are perpendicular to the direction of the primary channel flow; the velocity of the Dean flow varies across different parts of the channel, with nearly a zero value at the vortex core (54). As a consequence of the combined effect of the two size-dependent forces—the inertial lift force ($F_L \propto a_p^4$) and the additional Dean drag force ($F_D \propto a_p$)—particles with diverse diameters display different focusing degrees at distinct lateral positions across the width of the channel when flowing through the same curved microchannels. A detailed understanding and physical modeling of complicated particle-focusing behaviors remains a fascinating, yet still unfinished, research topic (7, 52, 55).

By taking advantage of diverse particle-focusing behaviors in inertial microfluidics, various cell- or particle-separation devices have been developed, and these are grouped into two different categories: those involving equilibrium and those involving kinetic separation (55). For equilibrium separation, the performance of cell sorters mainly relies on the accurate focusing of both targeted and nontargeted cells at distinct locations in the curvilinear microchannels. Separation into 3 different particle sizes (10, 15, and 20 μm) (56) and separation into 4 different sizes (7.32, 9.92, 15.02, and 20.66 μm) (57) have been reported to have high efficiency (90%) using spiral microchannels with strategically placed outlets. In one study, Lee et al. (58) employed a spiral system with multiple outlets to synchronize mammalian cultures and reported relatively high efficiency and throughput (approximately 15×10^6 cells/h). However, there was a trade-off between throughput and separation efficiency. When the concentration of cells in the microchannel is increased, cell–cell interactions are normally increased, causing expansion of the focusing band and affecting separation efficiency. To address this issue and further increase separation throughput, several recent studies (20, 59, 60) have explored the effect of the shape of the channel cross-section on the performance of spiral cell sorters. These studies discovered that by using channels with trapezoidal cross-sections (instead of those with conventional rectangular cross-sections) the distance between the equilibrium positions of large and small particles can be increased, thus facilitating better separation. It

Figure 2

(*a*) Separation using deterministic lateral displacement (DLD). Fluorescent micrographs of the trajectories of micron-sized particles inside a microfluidic DLD system with one input and two outputs (collection and waste) for enrichment of circulating tumor cells (CTCs). Panel *a* adapted from Reference 45 with permission from the American Institute of Physics. (*b*) Principle of hydrodynamic particle separation. (*i–iii*) Schematics showing particle positions at branching points using different flow rates. (*iv*) Schematic showing particle concentration and separation into multiple side channels. Panel *b* adapted from Reference 49 with permission from the Royal Society of Chemistry. (*c*) Schematic of particle separation using a spiral microchannel with a trapezoidal cross-section. At the outlet of the spiral microchannel (the A-A cross-section), CTCs are focused near the inner wall due to the combination of inertial lift force and Dean drag force at the outlet; white blood cells (WBCs) and platelets are trapped inside the core of the Dean vortex, which is formed closer to the outer wall. Panel *c* adapted from Reference 20 with permission from the Royal Society of Chemistry. (*d*) Schematic of particle focusing and separation using inertial microfluidics in straight microchannels. Inertial lift (F_L) acting on large particles (red blood cells) leads to differential migration to equilibrium positions; unfocused small particles (bacteria) exit from all outlets. Panel *d* adapted from Reference 19 with permission from Wiley. (*e*) Schematic of a microhydrocyclone structure, flow profile (V_a, V_c, and V_t are, respectively, the axial, radial, and tangential velocities), and different forces (the centrifugal force, F_c; the drag force, F_d; and the buoyancy force, F_b) acting on the particle in a trajectory. The inlet velocity initiates a rotational pattern that creates a downward spiral in the feed chamber. Centrifugal forces push the cells or particles that have higher specific gravity out toward the cone wall; these are then ejected at the bottom of the cone under flow. The remainder of the fluid travels upward and exits through the overflow. Panel *e* adapted from Reference 74 with permission from the American Society of Mechanical Engineers. (*f*) Schematic of the working mechanism of a microfluidic counterflow centrifugal elutriator. (*i*) Rotation-driven flow containing cells is introduced into the microchannel. (*ii*) In the separation chamber, particles remain at specific positions where the fluidic and centrifugal forces are balanced. (*iii*) Particle recovery is achieved by gradually increasing the fluid density. Panel *f* adapted from Reference 76 with permission from the Royal Society of Chemistry.

has been shown that spiral devices with a trapezoidal cross-section can provide better capacity for isolating small particles (i.e., they can be isolated near the outer wall where there is a strong Dean vortex) and achieve higher throughput, making this design ideal for concentrating large low-abundance target cells from highly abundant, small background cells. One such application is leukocyte isolation; Wu et al. (59) have demonstrated direct separation of human leukocytes from diluted blood (1.5% hematocrit) at a throughput of 1.33×10^8 cells/mL with approximately 96% separation efficiency. In a recent study, the same group employed spiral devices with trapezoidal cross-sections to enrich CTCs from blood (**Figure 2*c***). They reported successful recovery of more than 80% of viable cancer cells from 7.5 mL of RBC-lysed blood in 8 minutes, with extremely high purity (approximately 4 log depletion of WBCs); they also showed 100% positive CTC extraction from samples ($n = 10$) from patients with advanced metastatic breast and lung cancer (20).

Equilibrium separation has also been implemented in straight channels by coupling shear-induced lateral particle focusing with the sterically induced axial alignment of large particles in a pinched flow. In the work of Bhagat et al. (61), a pinched straight channel that had a pinching width comparable to the size of a CTC has been used to isolate spiked CTCs from 2% hematocrit blood at 0.4 mL/min (Reynolds number = 100), resulting in greater than 80% cell recovery along with a 3.25×10^5-fold enrichment over RBCs and 1.2×10^4-fold enrichment over leukocytes.

Kinetic inertial separation, however, takes advantage of the differential lateral migration between desired and undesired particles that occurs due to differences in net lift forces. Particles migrate and focus to their equilibrium positions only when there is sufficient channel length and time. Using this principle, Wu et al. (62) removed bacteria from 10% volume/volume (v/v) human RBCs by capitalizing on the greater lateral displacement of the RBCs caused by a stronger wall-induced lift effect. Their device was able to offer up to 99% purity with 60% separation recovery. However, this device was unable to work with whole blood due to extensive RBC cell–cell interactions. The flow rate of 2–18 μL/min also meant that processing time might be long for large sample volumes. Mach & Di Carlo (19) tried to overcome the limitations of sample volumes by creating a parallelized blood filtration device that had the potential to extend the application to treat neonatal sepsis (**Figure 2*d***). The device was able to process 30 mL of 0.5% v/v blood at 8 mL/min.

In addition to a straight microchannel, a spiral channel can also be used to perform kinetic inertial separation in Dean flow fractionation (DFF). The typical DFF device has a two-inlet two-outlet configuration. At the inlet region, the input cell mixture is confined to the outer half of the channel cross-section by introducing a cell-free sheath flow. Due to the Dean drag force, as cells pass through the curvilinear channel, they follow the streamlines and migrate laterally across the channel cross-section. For cells that are larger than the critical focusing threshold, lateral migration stops when they reach their equilibrium positions near the inner wall of the channel; smaller cells that do not have stable equilibrium positions travel with the Dean flow, displaying a back and forth lateral movement across the width of the channel. Using a DFF design, Hou and colleagues (63) developed a novel spiral biochip that is capable of processing blood (approximately 20–25% hematocrit) at a speed of 3 mL/h for isolating CTCs through a two-stage cascade system. The team also recently reported on a multiplexed version of their biochip, which is capable of processing lysed blood samples 15 times faster than the earlier version (that is, 7.5 mL blood in less than 10 minutes) (64). The clinical usability of their multiplexed biochip was demonstrated when it detected putative CTCs from 100% of blood samples ($n = 56$) collected from patients with advanced stage metastatic breast and lung cancer with high CTC purity—that is, a reduced number of contaminating WBCs were isolated with the CTCs (65).

In general, inertial cell sorters are the simplest microfluidic platforms that can separate cells with high throughput and with negligible effects on cell viability, genomic profile (66), and

immunophenotype (59). Although inertial microfluidics has inherent limitations in throughput arising from the defocusing phenomenon that occurs as a consequence of interparticle interactions, its high operational, volumetric flow rates mitigate this limitation. Moreover, the simplicity of the channel architecture and the ability to operate independently from external force fields facilitate the parallelization and stacking of microchannels, thus boosting the throughput. The resulting throughput surpasses that of most other techniques by orders of magnitude and could reach a value comparable to that of conventional bulk-scale cell-separation methods, thus giving inertial cell sorters the ability to rapidly screen large sample volumes (67–69).

2.2.4. Centrifugal methods (operation at high Reynolds numbers): hydrocyclones, counterflow centrifugal elutriation, and disk microfluidics. Hydrocyclones are important macrodevices used to separate solid–liquid suspensions in many mining and industrial processes (70). Without any moving parts, hydrocyclones separate suspended particles from fluid via centrifugal sedimentation (**Figure 2*e***); they have low capital costs and low maintenance costs (71). Hydrocyclones have been proposed recently as a means for separating cells in perfusion bioreactors (72) or during alcohol fermentation by yeast cells (73). However, these applications have precipitously worsened the separation efficiency for particles below certain sizes (approximately 10–15 μm). Since this size range covers several important cell types, recent efforts have been directed toward optimizing hydrocyclones to enable them to separate smaller particles. Bhardwaj and colleagues (21, 74) developed a microfluidic microhydrocyclone for separating micron- and submicron-sized solid particles. The effects on isolation efficiency related to parameters such as the diameter of the vortex finder and particle size were also investigated. Hwang et al. (75) studied particle sorting in hydrocyclones using mathematical models, and presented evidence that using a cone-shaped top plate could reduce the fine-particle circulation area and increase the efficiency of isolation.

Hydrocyclones are able to offer continuous particle separation at high throughput (that is, in liters per hour), which is much faster than any other described microfluidic particle-sorting technique. Due to their larger dimensions, hydrocyclones are also less prone to clogging, and, hence, provide a more reliable sorting technique. Nonetheless, the fabrication and operation of small-scale microhydrocyclones remain challenging. In addition, this technology relies on density differences between particles and fluid, limiting its applications to certain sizes of particles and cells.

Counterflow centrifugal elutriation (CCE) is another particle-sorting technique that was described as early as 1948 by Lindahl (77) for use in applications such as sperm sorting (78). This method exploits the balance between a centrifugal force and a counterflow drag force to separate particles based on differential sedimentation properties. Briefly, when particles first enter the CCE chamber, they are subjected to centrifugal force, and, thus, stay near the boundaries of the chamber. A buffer solution introduced in the opposite direction of the centrifugal force provides a varying counterflow drag force, based on its flow rate, to push the particles toward the center of the chamber. When the drag force becomes stronger than the centrifugal force (due to the increasing rate of the buffer's flow), the particles or cells exit the chamber, with smaller particles or cells exiting before larger ones.

CCE has become well established for particle sorting and cell-cycle synchronization. Readers can refer to reviews by Grosse and colleagues (79) for information about macroscale CCE applications. Banfalvi (80) has used CCE for cell synchronization because CCE does not disturb cell-cycle progression, and highly synchronized cell populations can be obtained especially in the G_1 phase, and early and mid-S phase. Although this technique has been extensively used in the macroscale, microfluidic CCE was recently used by Morijiri et al. for Jurkat cells (76) and blood-cell separation (81). The team modified the conventional CCE method to isolate particles, but

included two types of fluid with different densities for stepwise elution of particles; they also used a branched loading channel to minimize clogging and improve particle focusing to the center of the CCE chamber (**Figure 2*f***). Using the device, Morijiri and coworkers were able to isolate 98% of RBCs from WBCs (81). The authors also concluded that cell size is the most important factor in their separation processes when compared with other parameters, such as shapes and densities. Nonetheless, a 10× dilution of blood was necessary to improve separation resolution. In addition, the introduction of fluids with different densities also necessitated two different reservoirs, making the entire system more complex to fabricate. Similar to the hydrocyclone, CCE is also a label-free separation technique that is based on the inherent physical properties of samples such as size and density. However, miniaturized CCE systems cannot be employed for large-volume sample processing due to physical restrictions necessary in the design (i.e., for optimum operation) and the concentration of the input sample (82, 83).

Centrifugal microfluidics is a new class of miniaturized systems that has been used in cell-based applications for molecular separation, mixing, reaction, and detection. This technique is also referred to as rotational centrifugal microfluidics because unlike the flow in spiral channels, centrifugal forces are induced not by bends in the channels but by the actual rotation of the platform (84). [Ducrée et al. (85) provide additional detail on the physics of centrifugal particle focusing.] Centrifugal microfluidics has proven to be a suitable blood-separation technique because it exploits the higher density of blood cells compared with the density of plasma. For example, Haeberle and colleagues (86) extracted 2 mL of plasma with 99% purity from 5 mL whole blood in 20 s using a centrifugal microfluidic platform. They also found that the purity of the plasma was unaffected by the frequency of rotation, thus increasing the robustness of this plasma-extraction system. Zhang et al. (87) created a centrifugal microfluidic platform with a curved geometry to induce additional centrifugal effects to obtain cell-free plasma. In this system, RBCs, which have a higher density, migrate away from the center of the microchannel toward the outer curved wall. The team achieved an RBC separation efficiency of 99% with an input blood sample with 6% hematocrit and 65% with a 48% hematocrit input; the differences were due to differences in blood viscosity and cellular interactions. However, the efficiency of plasma collection was approximately 24% and throughput was only 15–30 μL/min. The same team then improved the design of the platform by incorporating an out-of-plane microvalve (88) to prevent blood cells from diffusing from the sedimentation reservoir to the plasma reservoir at a critical rotational speed, and achieved 99.9% plasma purity with 96% plasma yield with their new design. Shiono and colleagues have also applied centrifugal devices to isolate different types of blood cells, such as nucleated blood cells from RBCs (89), lymphocytes from neutrophils, cultured human mast cells from fibroblasts (90), and human hematopoietic progenitor cells from peripheral and umbilical cord blood (91). Their devices are made up of six parallel fluid streams, and cell separation occurs owing to the differential densities of the cells.

There are other uses of centrifugal microfluidic platforms in particle sorting. For instance, Martinez-Duarte and coworkers (92) made use of carbon electrodes to induce dielectrophoresis (DEP), and then combined this with a centrifugal compact disc (CD) platform to separate yeast cells from latex beads with 100% efficiency at a flow rate of 5 μL/min.

The advantages of using a centrifugal microfluidic platform are that such a system requires minimal instrumentation to perform fluid propulsion because only rotational motion is needed, and there is no need for external syringe pumps. The absence of external interconnects also creates a complete fluidic network, thus minimizing the formation of bubbles that typically perturb the flows in inertial microfluidic platforms. It is equally important to note that centrifugal pumping is not strongly affected by the physicochemical properties of fluids, such as ionic strength and pH (93), and does not require high voltage for operation (94). Through experimental validation, it

has also been found that flow rates for different types of biological fluids, such as urine, blood, and plasma, can range from 5 nL/s to 0.1 mL/s, with a rotational speed ranging from 400 to 1,600 rpm, channel widths from 20 to 500 μm, and channel heights from 16 to 340 μm (95). These advantages of centrifugal microfluidic platforms lend these systems to a wide range of biomedical particle-sorting applications.

2.3. Affinity-Based Techniques (Magnetophoresis)

Affinity-based cell sorting generally refers to the commonly used techniques of fluorescence-activated cell sorting (FACS) and magnetic-activated cell sorting (MACS), both of which make use of antibodies specific to targeted cells to isolate them (positive enrichment) or unique to unwanted cells to remove them (negative enrichment). FACS separation is achieved using laser excitation of fluorophores bound to the desired cells, with excitation above a threshold level signaling the cell to be separated (10, 96). FACS has been the workhorse of the biological and pharmaceutical industries due to its mature development, sensitivity, throughput (approximately 100,000 cells/s), and ability to track multiple parameters (97). Recently, researchers have tried to incorporate FACS into microfluidic platforms (i.e., FACS-on-a-chip). However, the throughput of microfluidic flow cytometers is not high enough to compete with the throughput of commercial systems (98).

In MACS, immunomagnetic isolation is usually performed using magnetic microbeads coated with monoclonal antibodies or ferrofluids. A strong magnetic field is then used to isolate the magnetic beads that are attached to the desired cell population. In contrast to FACS, magnetic cell sorting can be operated in either a serial or a parallel manner, resulting in remarkably high throughput. Enrichment of up to 10^{11} cells in less than 30 minutes has been reported (10, 99). In the context of microfluidics, MACS has been employed widely by many researchers for high-throughput cell separation (100). For example, Hoshino et al. (22) presented an immunomagnetic microchip (**Figure 3*a***) in which magnetically tagged CTCs were captured inside a magnetic-field gradient in microfluidic channels. They reported up to a 90% capture rate, even with a flow rate of 10 mL/h.

IsoFlux (Fluxion Biosciences, South San Francisco, CA) is a newly developed microfluidic platform (101) that has microfluidic channels in which cells tagged with magnetic particles are exposed to highly uniform and concentrated magnetic fields that enable more efficient recovery of the target cells. Also, Kang and colleagues (102) have reported on the development of a microfluidic–micromagnetic cell-separation device that has been developed to isolate, detect, and culture CTCs from whole blood. In addition to isolating cancer cells, the same group used immunomagnetic microbeads and microfluidics to cleanse extracorporeal blood (**Figure 3*b***) to selectively remove pathogens from contaminated blood with an efficiency of around 80% at a flow rate of 20 mL/min (103).

Given the lack of agreement on CTC surface markers (104), negative enrichment platforms that remove unwanted subpopulations, such as leukocytes, have been developed to avoid losing CTCs that lack conventional CTC markers [e.g., CTCs without epithelial cell adhesion molecules (EpCAMs)] (105, 106). In a recent study, Chen et al. (107) demonstrated the use of a microfluidic disk-based separation device for enriching CTCs using immunomagnetic negative selection with a multistage magnetic gradient on the disk. Their device recovered more than 60% of spiked cancer cells and removed more than 99.96% of WBCs.

Another example of an affinity-based particle sorting technique uses supermacroporous cryogels (108). These gels have large interlinking pores, with dimensions in the range of 10–100 μm. Ligands specific to cells may be added to the gels, allowing the targeted cells to be isolated while other cells flow through the cryogel column without being retained. Owing to the high elasticity

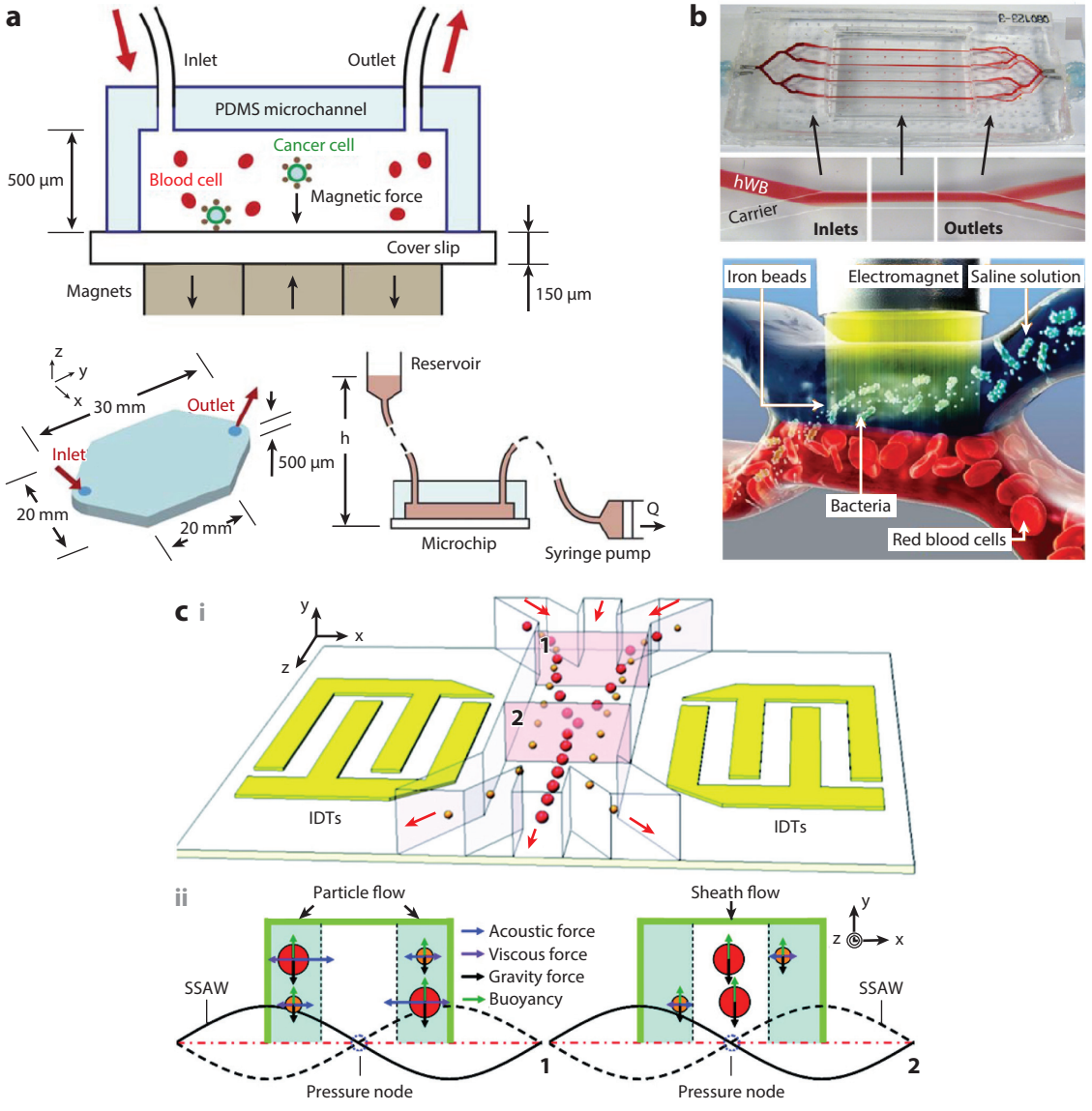

Figure 3

(*a*) Schematic of a microfluidic chip for immunomagnetic detection and separation of circulating tumor cells (CTCs). CTCs in blood are labeled with magnetic particles functionalized with EpCAM (epithelial cell adhesion molecule), and captured by the magnetic field as the blood flows through the microchannel at a rate of 2.5–10 mL/h. Panel *a* adapted from Reference 22 with permission from the Royal Society of Chemistry. (*b*, *top*) Optical image of a micromagnetic–microfluidic blood-cleansing device made from polydimethylsiloxane (PDMS). (*Bottom*) Schematic illustrating the mechanism of operation. The modified immunomagnetic microbeads are used to cleanse *Candida albicans* fungi from flowing human whole blood (hWB); the fungi are a leading cause of sepsis-related deaths. The device generates magnetic-field gradients across vertically stacked channels to enable continuous separation of fungi from flowing whole blood. Panel *b* adapted from Reference 103 with permission from the Royal Society of Chemistry. (*c*) Schematic illustrating the principles of acoustic separation using standing surface acoustic waves (SSAWs). The acoustic forces are generated using interdigital transducers (IDTs); these forces reposition the larger cells closer to the center of the channel and smaller cells farther from the center, thus allowing continuous separation at the outlets. Panel *c* adapted from Reference 112 with permission from the Royal Society of Chemistry.

of the cryogels, absorbed cells can be detached using mechanical compression. Detached cells have also been shown to be highly viable and able to be cultured. In addition to blood cells, bacteria such as *Escherichia coli* have also been shown to adsorb onto cryogels. These bacteria can also be detached from the matrices for culturing (108, 109). However, some common problems with this technique are fouling of the column, nonspecific adsorption, and possible damage to cells due to the high shear rate from the high flow rate (110). The surface area of the binding beads, as well as the strength of the binding, may also limit the effectiveness of cryogels.

Although affinity-based techniques, using either positive or negative selection, are well established and widely practiced, it is important to understand the inherent limitations of these techniques. For example, there are often limits to using cells captured by positive selection for downstream assays, especially functional assays, such as colony formation or culture. Also, the efficiency of separation is almost solely determined by the quality of the capture agent used, requiring reliable high-quality capture agents, such as antibodies. And, especially for applications requiring high-volume processing, the cost of capture agents could be significant and prohibitively high.

2.4. Acoustophoresis

Acoustophoresis uses high-intensity acoustic radiation to separate particles (111). It has long been known that particles, such as cells suspended in fluid, can be manipulated using high-intensity standing waves of sound, which are often produced using acoustic resonators. Particle or cell separation can be performed by creating standing waves over the cross-section of a microfluidic channel (112). The radiation force causes the particles to move toward either the pressure nodes or the antinodes of the standing wave. There are comprehensive and insightful reviews of using bead-based immunoassays with acoustophoresis (113), of creating microscale systems for particle sorting using standing waves (50, 114), and of clinical applications for this particle-sorting technique (115).

Petersson and colleagues (116) used free-flow acoustophoresis to separate differently sized beads (2–10 μm) as well as to separate blood into platelets, RBCs, and WBCs. Several groups also have provided suggestions about ways to improve acoustophoretic particle sorting in microfluidic channels (50). A stronger acoustic radiation force can be generated in microscale, leading to better performance of particle separation. In one study, Persson et al. (117) also used acoustic radiation forces to demonstrate the automatic selection of bacteria from libraries. Lenshof and colleagues (118) developed an integrated system combining acoustophoresis and a microarray chip coated with prostate specific antigen to remove blood cells. Their system generated 12.5% clean plasma by volume (55–60% of total blood is plasma), with approximately 99.99% depletion efficiency for RBCs. Dykes and coworkers (119) managed to utilize ultrasonic standing waves to remove platelets from samples of peripheral blood progenitor cells. Thévoz et al. (120) reported using acoustic radiation forces for cell synchronization. Their device exploits the differential cell sizes present during different cell cycles. The team achieved 84% synchrony in the G_1 phase and a throughput of 3×10^6 cells/h per microchannel. Augustsson and team (121) demonstrated that sorting fixed and viable cancer cells is possible by creating ultrasonic resonances in temperature-stabilized microchannels. In their work (121), prostate cancer cells were isolated from WBCs with a recovery rate of up to 93.9% and a purity rate of up to 99.7%. The isolated cancer cells were viable and could be cultured. Similarly, Yang & Soh (122) isolated MCF-7 cells from a mixture of viable and nonviable cells (10^6 cells/mL) using acoustic radiation forces at flow rate of 12 mL/h.

In addition to medical applications, acoustophoresis has been useful in industry as well. Shi and coworkers made use of standing surface acoustic waves (SSAWs) that are able to separate particles based on differences in volume, density, and compressibility (112, 123). Their device was able to achieve 80% efficiency in separation (**Figure 3*c***). Grenvall et al. (124) created a microfluidic device

that uses a multinode standing wave to concentrate lipid emulsions from raw milk samples, and, thus, preconditions the sample for downstream analyses of the protein and lipid contents. A lipid depletion efficiency of approximately 90% has been achieved using their system. Ultrasonic sorters have also been used widely in the pharmaceutical industry to separate and recycle mammalian cells for use in bioreactors (125).

Acoustophoretic particle sorting can be performed without labels and physical interactions. This minimizes physical and biochemical damage to cells (e.g., damage to gene-expression profiles). Acoustophoretic particle sorting can also be extended to the separation and concentration of bacteria and even nanoparticles (126). However, the presence of external elements, such as a resonator and function generator, makes their fabrication and use complicated. It is also crucial to note that this technique depends strongly on the size, volume, and density of the particle, which can be confounding factors for harvesting target cells of similar phenotypes but with slightly different sizes (127).

2.5. Biomimetic Separation

Biomimetic separation uses naturally occurring hemodynamic phenomena in microvasculature, such as plasma skimming and cell margination, to separate various blood components. Even old ideas about hemodynamics can be further engineered in a microfluidic platform to provide enhanced or novel functionalities by modifying the geometry and increasing the flow rate. These mechanisms typically use raw, undiluted blood (40–50% hematocrit), and, therefore, achieve high cell-processing rates and allow direct processing of raw blood, both of which are ideal features for applications in blood diagnostics and therapeutics.

At the heart of these mechanisms are the unique viscoelastic properties of RBCs, the major fluidic component of blood. In these techniques, RBCs are placed under a shear gradient typically found in blood microvessels, and this drives them toward the axial center of the channel or vessel, creating a cell-free layer near the vessel wall and reducing effective fluidic resistance (known as the Fåhræus–Lindqvist effect) (128). Such a cell-free layer can be harvested at bifurcation points in blood vessels or microchannels (the Zweifach–Fung effect), and potentially used for plasma and cell separation. Geng et al. (129) combined the bifurcation law, centrifugation, and the diffuser-nozzle effect to isolate plasma with an efficiency of 95%. Nevertheless, the flow rate was only 0.06 μL/s even after the blood had been diluted to 20 times the original volume. Jäggi and coworkers (130) then tried to improve the flow rate to milliliters per minute by extending the height of the channel. The team also investigated the critical flow rate needed to obtain a pure plasma stream at various hematocrit levels. They found that at higher hematocrit levels (i.e., 45%, which is a physiological level), the separation efficiency of their devices decreased significantly, falling to approximately 30%. This effect, often referred to as plasma skimming, is an ideal method for harvesting cell-free plasma, which is required for many blood-based tests used to detect biomarkers. Yang et al. (131) created a microfluidic device with a high ratio of the flow rate in the main channel to the rate in the branch channel (>6:1), and collected 15–25% of the plasma volume. The device was able to function when used with whole blood and caused minimal hemolysis due to the low flow rate of 10 μL/h. Faivre and colleagues (132) also used in vitro plasma skimming to create cell-free plasma. They reported that sudden channel expansion could enhance the cell-free layer and lead to isolation of close to 24% of the initial plasma volume. Sollier et al. (133) managed to isolate 10.7% of plasma from 20× diluted blood at a flow rate of 100 μL/min. The purity was also comparable to that of methods such as centrifugation.

Margination describes another in vivo process in which less deformable cells are crowded out toward the periphery of the microvasculature as a result of the more deformable (or fluid-like)

RBCs concentrating at the center of the vessel. Shevkoplyas et al. (134) made use of this phenomenon to isolate leukocytes from RBCs. Their device was able to enrich leukocytes by 34-fold over the RBC count. The use of a combination of multiple symmetric and asymmetric channels improved the leukocyte count from 4,300/μL to 42,300/μL. Hou and colleagues (24) also used margination to isolate malaria-infected RBCs from whole blood. Infected RBCs are known to be less deformable than uninfected RBCs, and, therefore, the infected RBCs migrate to the peripheral outlets where they can be collected for downstream analyses (**Figure 4*a***). Using the same phenomenon, the team developed a novel microfluidic device to enable label-free removal of both microbes and inflammatory cellular components (platelets and leukocytes) from whole blood. Using a cascading system, they have shown a flow rate of up to 6 mL/h (135).

2.6. Integrative Systems

Integrative systems capitalize on the advantages of different particle-sorting techniques. For instance, Sollier and coworkers (138) recently reported on a high-throughput microfluidic device that can be used for ultrahigh-throughput separation of CTCs (20 minutes to process 7.5 mL of whole blood) and uses a combination of inertial focusing and vortex technology, capitalizing on previous findings by Hur et al. (136). The straight channel that is upstream from the vortex reservoir focuses cells to their equilibrium positions. Upon entering the vortex reservoir, the wall-induced lift forces become negligible and the stronger, shear-gradient lift forces cause larger particles to be trapped in the vortices in the reservoir (**Figure 4*b***). Small particles are removed by washing, and large particles are released by slowing the flow rate. Wang et al. (139) made use of similar principles to isolate polystyrene beads for particle sorting and blood fractionation. Song & Choi (140) also provided a proof of concept by combining hydrophoretic and inertial effects to show that particles can be sorted based on size in a label-free sheathless system using relatively high flow rates (10^6 cells/h per channel). Adams et al. (141) demonstrated that acoustic and magnetic particle sorting can achieve a throughput of 20 mL/h. Liu and colleagues (142) combined DLD and an affinity-based technique to isolate breast cancer cells with 90% efficiency at a flow rate of 9.6 mL/min. Seo and colleagues (143) have shown that combining magnetophoresis (i.e., by employing the magnetic properties of blood cells) with hydrodynamics (using the momentum of particles) can be useful for label-free cell separation (0.5 mL/min). In an interesting study, Hur et al. (66) made use of the balance between deformability-induced lift force and inertial lift forces to classify cells. The size, elasticity, and viscosity of particles affected their lateral displacement as they flowed through a microchannel. Remarkably, the lateral equilibrium positions of malignant MCF-7 cells could be clearly distinguished from those of benign MCF-7 cells, hinting at the possibility of determining cancer-stage progression.

Another excellent example of an integrative system is the CTC-iChip (**Figure 4*c***), which combines DLD, inertial focusing, and magnetophoresis to sort rare cells (25, 144). The device made use of anti-CD45-covered superparamagnetic beads to remove WBCs via the negative-depletion principle. There are two stages of separation in this technique: DLD is used in the first stage to separate CTCs from WBCs, and this is followed by the second stage in which inertial focusing and magnetophoresis are used to remove WBCs. The CTC-iChip offered up to 97% yield of CTCs, with a processing speed of 8 mL of whole blood per hour. In another interesting study, Moon et al. (137) successfully combined multi-orifice flow fractionation (MOFF) and DEP cell separation techniques in a serial manner to enrich MCF-7 cells at a flow rate of 126 μL/min. MOFF allowed for high-throughput separation while DEP enhanced the efficiency of the separation. RBCs and WBCs were depleted with efficiencies of 99% and 94%, respectively (**Figure 4*d***).

3. CASE STUDIES OF LARGE-VOLUME MICROFLUIDIC DEVICES: DIAGNOSTICS AND THERAPEUTICS

3.1. Rare-Cell Enrichment and Analysis of Large Sample Volumes

The ability to isolate low-abundance target cells (those occurring at <1,000/mL) from a pool of heterogeneous nontarget cells, and the subsequent characterization of those cells, are highly valuable in many applications, such as prenatal diagnosis (e.g., enriching fetal cells in maternal blood), cancer research (e.g., isolating CTCs from peripheral blood to perform a liquid biopsy), and stem cell therapy (e.g., separating stem cells from peripheral or cord blood, or bone marrow) (145). Microfluidic platforms are ideally suited for handling and analyzing a small number of cells, and offer precision that is not possible with conventional fluid-handling systems (e.g., microwell plates and pipettes). Yet, in order to isolate a sufficient number of target cells from these samples,

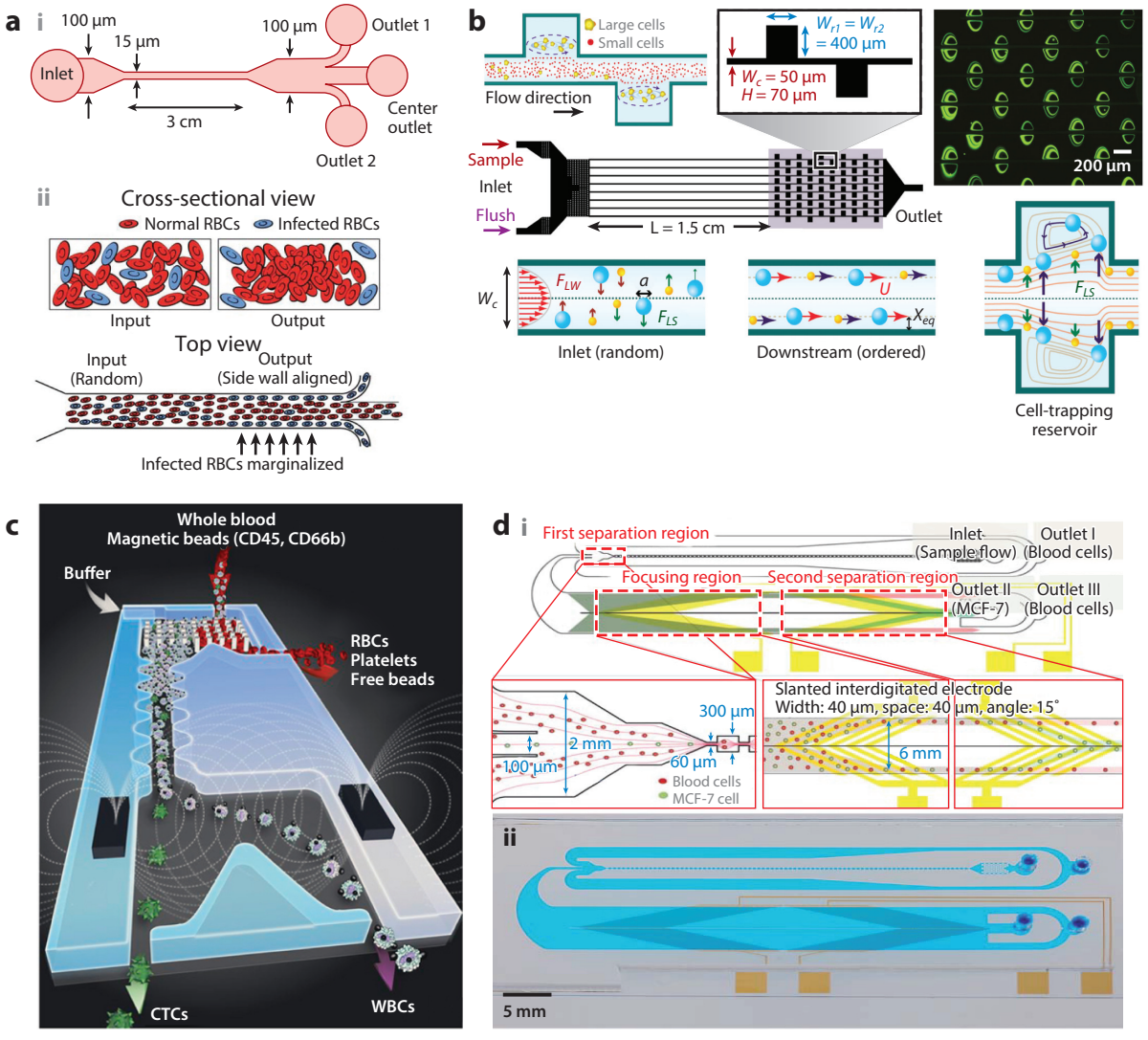

it is necessary to process a large volume (approximately 1–20 mL or even more) of raw sample, a capability that became available in the field of microfluidics only recently.

In the context of cancer research, CTCs have attracted extensive attention, and functional analyses of CTCs have been used for real-time liquid biopsy in cancer management (146). The detailed characterization of CTCs holds the promise of enabling the optimal therapy to be chosen for individual patients during the course of their disease. However, sufficient numbers of CTCs are required to obtain a representative picture. Although most clinical studies are performed using just 7.5 mL of blood from a patient, recent studies have shown that it is necessary to process larger volumes of blood to obtain enough cells for reliable enumeration and assessment of their proteomic and genomic profiles to help select an effective therapy for particular patient. Although in vitro expansion of CTCs (147) could alleviate this issue, there is a concern that such expansion might also change the original biochemical and phenotypic states of the original CTCs obtained from the patient.

Although increasing the volume of a sample is clearly one of the most effective ways to enrich more putative CTCs, clinical considerations about patients' health impose an upper limit in the amount of blood that can be extracted from one patient. Isolating CTCs in vivo provides an elegant way of bypassing this limitation. Saucedo-Zeni et al. (148) recently developed an in vivo CTC detector by functionalizing the surface of a gold-plated Seldinger guide-wire with anti-EpCAM-engrafted polycarboxylate hydrogel. By inserting the detector into the patient's cubital vein, up to 1.5 liters of blood could pass through the 2-cm-long functionalized area of the detector within 30 minutes, thus capturing a significantly higher number of CTCs. Moreover, the gold galvanization and hydrogel coating on the detector's surface greatly improved the specificity of CTC detection by minimizing the nonspecific binding of other blood components. Currently, a multicenter clinical trial is being undertaken to verify the applicability of this technique for patients with high-risk prostate cancer (European Research Area Network on Translational Cancer Research). The performance of this type of positive-selection CTC capture relies heavily on the choice of capture marker (or markers) and the quality of the capture agents. Thus, EpCAM-based methods of CTC capture could result in target cells escaping if CTCs are undergoing epithelial-to-mesenchymal transition, along with a coincident loss of EpCAM expression

Figure 4

(*a*, *i*) Schematic of a biomimetic microfluidic chip for separating malaria-infected red blood cells (RBCs) from healthy cells in a continuous fashion. (*a*, *ii*) Schematic of the cross-sectional and top views of the device showing the separation mechanism. The randomly distributed infected RBCs (*blue*), which are less flexible than normal RBCs, migrate to the channel's side walls as the flow reaches the outlet; they are then filtered out using a three-outlet system. Panel *a* adapted from Reference 24 with permission from the Royal Society of Chemistry. (*b*) Schematic of a high-throughput microfluidic system for cell separation that uses inertial and vortex technologies. The device consists of 8 parallel, straight channels (50 × 70 μm) with a high aspect ratio; each channel has 10 cell-trapping reservoirs (400 × 400 × 70 μm). Larger cells are trapped in the reservoirs while smaller cells freely pass through due to differences in lift forces (the wall-induced lift force, F_{LW}; the shear-induced lift force, F_{LS}), and are separated at the end of the process. U is the fluid velocity, and X_{eq} is the equilibrium distance of particles from the channel's side wall. Panel *b* adapted from Reference 136 with permission from the American Institute of Physics. (*c*) Schematic of circulating tumor cell (CTC)-iChip. This hybrid chip is composed of a deterministic lateral displacement section at the entrance that isolates nucleated cells from whole blood using size-based exclusion; this section is followed by an inertial focusing section that is used to line up cells to prepare for precise separation by a magnetic field. Panel *c* adapted from Reference 25 with permission from Nature Publishing Group. (*d*) Schematic illustrating the working principles of a hybrid microfluidic chip combining dielectrophoresis (DEP) and inertial focusing to separate cancer cells from blood. (*d*, *i*) In the first separation region, inertial forces are used to separate the relatively larger cancer cells from blood cells (although separation efficiency is not 100%); the cancer cells then enter the wider zone, which is embedded with electrodes; in this area, the cells are subjected to positive DEP, which further separates the cancer cells from contaminated blood cells. (*d*, *ii*) Optical image of the fabricated device. Panel *d* adapted from Reference 137 with permission from the Royal Society of Chemistry.

(104). Additionally, the types of downstream assays that can be used on captured CTCs are often limited, and results might be skewed due to the strong interaction between CTCs and the capture agents. An alternative approach is to isolate CTCs through extracorporeal blood salvage so that CTC-free blood, particularly RBCs, is returned to the patient. Eifler et al. (149) investigated the applicability of using a sequential process of leukapheresis followed by elutriation to isolate CTCs from high-volume samples ex vivo. First, the authors harvested mononuclear cells from 10 liters of blood using leukapheresis; they then spiked in the cancer cells at a frequency of 26 cancer cells per 10^6 blood cells. Subsequently, they isolated the larger cancer cells via elutriation, and this was followed by antibody-based detection of cancer cells using FACS. The authors reported 66% ± 8% recovery and 58% ± 21% purity for the spiked cancer cells; they also reported recovery of more than 90% of mononuclear cells during the elutriation step. In a recent, comprehensive study, Fischer and colleagues (150) screened leukapheresis products generated from up to 25 liters of blood per patient in order to monitor CTCs; they successfully detected CTCs in more than 90% of samples from patients with nonmetastatic breast cancer, and found a median of 7,500 CTCs per patient. Although this approach may be useful for isolating CTCs that are present in high numbers, a high level of background WBC contamination (of approximately 10^5 to 10^6 WBCs per CTC) could compromise downstream analysis. Given this issue, Warkiani et al. (20) recently reported on an ultrahigh-throughput microfluidic system that can enrich putative CTCs from 7.5 mL of lysed blood in less than 8 minutes with very high purity (99.99% removal of WBCs). The same biochip also works for processing whole blood. Using a multiplexed version of the same biochip, one could easily process larger blood volumes with a throughput of approximately 50–100 mL/min with more than 90% recovery of CTCs (65). This elegantly demonstrates that a properly engineered microfluidic system can overcome the shortcomings of traditional cell-separation techniques and match or outperform traditional techniques in terms of throughput of volumetric flow. A European consortium, known as the Circulating Tumor Cells Therapeutic Apheresis group (or CTCTrap), is currently exploring new ways to enrich CTCs from peripheral blood by combining immunocapture and size-based separation techniques (**Figure 5*a***) (151).

3.2. Intraoperative Blood Salvage

Intraoperative blood loss is a dreaded complication of cancer surgery (152). An average of 2 liters of blood is lost during bone cancer surgery (153). Currently, this loss is replenished by allogeneic blood transfusion, which places an enormous burden on blood banks as well as exposing patients to risks related to blood transfusion, namely infection, immunosuppression, tumor progression, and transfusion reactions (154, 155). The alternative method for replenishing blood loss is intraoperative cell salvage (IOCS), a system in which blood lost during surgery is salvaged and returned to the patient instead of being discarded (156).

IOCS has not been used in tumor surgery because of the theoretical concern about returning CTCs to patients; however, for the past three decades there has been no concrete evidence that this occurs. On the contrary, a number of studies have supported the effectiveness of IOCS, especially when it is used in combination with leukocyte filters during tumor surgery or during other surgeries, including hepatobiliary, gynecological, gastrointestinal, and urological operations (157, 158). Despite evidence of the efficacy of using IOCS with leukocyte filters in cancer surgery, there are drawbacks to using these filters for blood salvaged during these procedures—that is, the filtered blood is rich in RBCs but may be devoid of WBCs. Theoretically, there would be a definite advantage to preserving WBCs to provide patients with immunogenic cells to fight against infection. Therefore, the need to develop an alternative low-cost technology for intraoperative

blood salvage that has the ability to deplete putative CTCs while returning the majority of blood cells (platelets, RBCs, and WBCs) is urgent, and opens up a new opportunity for the use of high-throughput microfluidic cell-separation techniques.

3.3. Extracorporeal Blood Purification for Sepsis Therapy

Cell separation for therapeutic interventions is another major field that requires an efficient, reliable, and high-throughput system in which microfluidic methods may offer great benefits. Sepsis therapy provides a typical example of the need to remove pathogens and even immune cells (159). Sepsis, systemic inflammation caused by severe microbial infection, is the leading cause of death in US intensive care units (160). To attenuate the overwhelming inflammatory response of the host, efforts have been invested in improving the outcomes of septic patients by using extracorporeal blood purification to remove cytokines and endotoxins. Although many extracorporeal blood-purification techniques have demonstrated efficacy in clearing these molecular targets from plasma, clinical studies have reported limited success in using molecularly targeted blood purification (159). However, it has also been proposed that blood-purification therapy should be used for a broader spectrum of targets, including microbial pathogens and host immune cells (161).

Recently, a number of microfluidic approaches have aimed to implement size-based and affinity-based removal of pathogens. In the former case, researchers took advantage of the size differences between typical microorganisms (approximately 1–3 μm) and human blood cells (>6 μm) to remove pathogens from the blood. Currently, the highest throughput reported for size-based separation of pathogens from blood cells is 240 mL/h with 0.5% v/v blood spiked with *E. coli*; this was obtained using a parallelized, inertial, microfluidic system (19). Despite the high throughput and high efficacy of pathogen removal (>80%), the necessary blood dilution prior to processing demands the use of a downstream hemoconcentrator, thus complicating the actual operation of this system. As an alternative approach, Yung et al. (103) developed an affinity-based system in which microbes were captured by magnetic microbeads coated with antibodies; these were then removed from the blood by magnetically pulling the beads into a waste stream flowing parallel to the blood sample. Using a multiplexed system, the authors reported pathogen clearance of more than 80% at 20 mL/h of whole blood in a single pass. The team claimed that higher throughput for human extracorporeal blood cleaning is possible using larger channels and more stacking. Because broad-spectrum pathogen removal is desired during sepsis treatment, researchers at the Wyss Institute have developed a capture agent similar to the human mannose-binding lectin (MBL), which is present naturally in the circulatory system and binds to almost all microbial classes (162). It is highly plausible that low-cost MBL-coated magnetic nanobeads could be used to cleanse whole human blood of infectious pathogens. However, caution must be exercised when considering the safety of this approach, particularly issues that may arise from the imperfect removal of magnetic nanobeads from patients' circulation.

Similarly, extracorporeal blood-purification platforms aimed at immune-cell removal have been developed mainly using affinity-based approaches that employ sorbent polymer (163) or synthetic biomimetic membrane (164). Rimmelé et al. (161) have shown that leukocytes together with cytokines can be adsorbed onto CytoSorb (CytoSorbents, Monmouth Junction, NJ), a type of polystyrene divinylbenzene copolymer bead. By passing blood through columns of CytoSorb beads for extracorporeal blood purification, the authors demonstrated reduced inflammatory factors, circulating neutrophils, monocytes, and platelets in an ex vivo study. However, most of these affinity-based blood-cleansing systems suffer from nonspecific binding and, more importantly, an increase in the local release of certain cytokines caused by enriching immune cells at capture

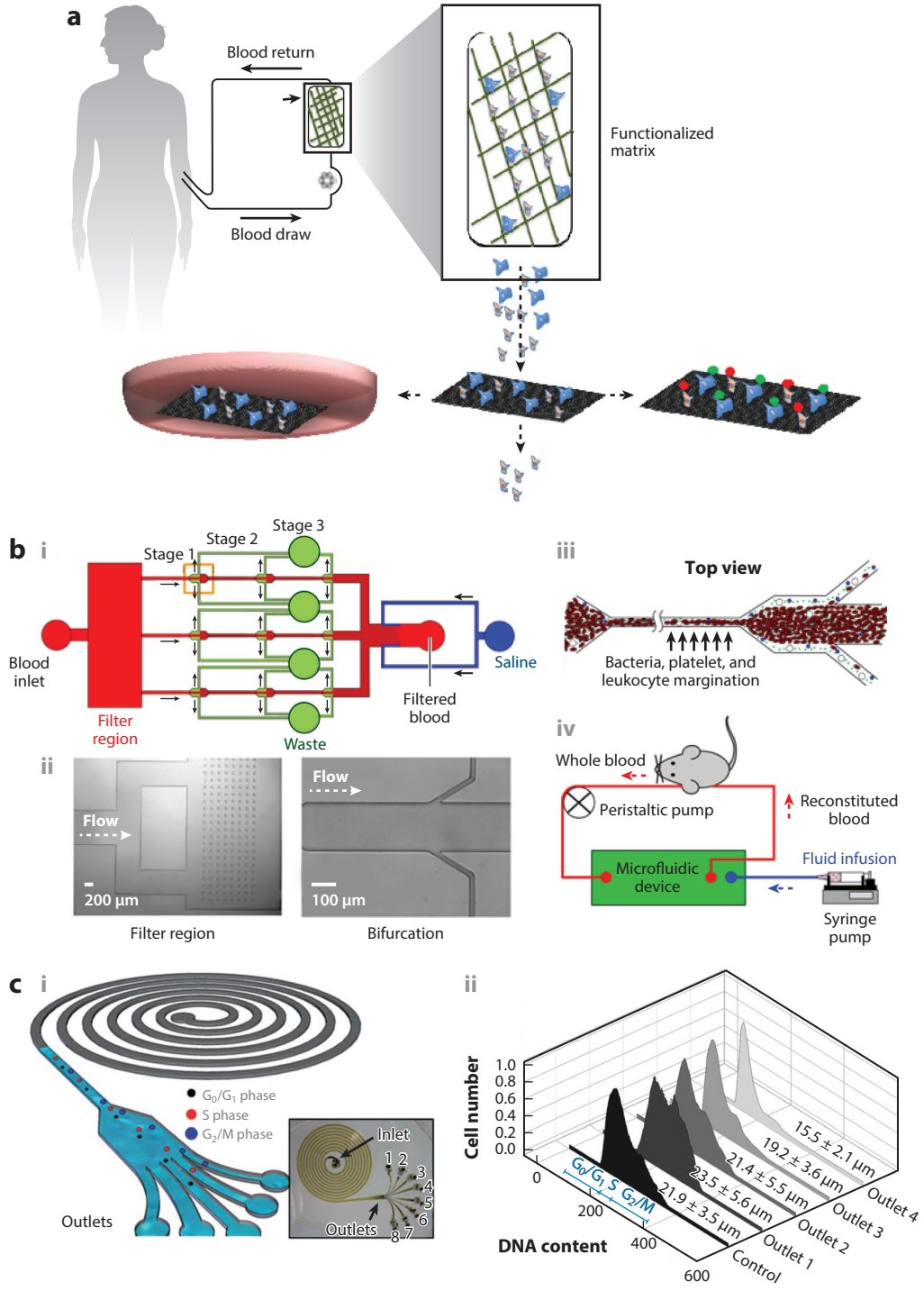
a
Blood return
Blood draw
Functionalized matrix
b i
Stage 1
Stage 2
Stage 3
Blood inlet
Filter region
Waste
Saline
Filtered blood
ii
Flow
200 µm
Filter region
Flow
100 µm
Bifurcation
iii
Top view
Bacteria, platelet, and leukocyte margination
iv
Whole blood
Peristaltic pump
Reconstituted blood
Microfluidic device
Fluid infusion
Syringe pump
c i
G0/G1 phase
S phase
G2/M phase
Outlets
Inlet
1 2 3 4 5 6 7 8
Outlets
ii
Cell number
1.0
0.8
0.6
0.4
0.2
0.0
0
200
400
600
DNA content
G0/G1 S G2/M
15.5 ± 2.1 µm
19.2 ± 3.6 µm
21.4 ± 5.5 µm
23.5 ± 5.6 µm
21.9 ± 3.5 µm
Outlet 4
Outlet 3
Outlet 2
Outlet 1
Control

sites (163). Alternatively, Hou et al. (165) developed a microfluidic blood margination (μBM) device for the nonspecific removal of inflammatory cells and microbes from whole blood. The μBM device, composed of straight channels with cascading bifurcations, was inspired by leukocyte margination, which is explained in Section 2.5 (166). The authors removed approximately 80–90% of pathogens, with more than 80% removal efficacy for platelets and leukocytes at a throughput of approximately 1 mL/h per channel. In a separate report using a murine model of sepsis, a flow rate of approximately 90–150 mL/h has been reported, with similar performance, using a 32-channel parallelized platform, thus demonstrating the feasibility of μBM as a purification approach in clinical settings (**Figure 5*b***) (167). However, it should be mentioned that in using the μBM approach, separation was usually accompanied by the loss of approximately 20% of blood in the waste channels; thus, additional fluid support may be needed during operation.

3.4. Wearable or Implantable Artificial Kidneys

The possibility of providing large-volume extracorporeal hemodialysis and peritoneal dialysis using miniaturized devices is also a major interest in the field of artificial kidneys, which could be widely applied as a therapy for kidney failure. Despite increasing evidence favoring prolonged or frequent dialysis treatment, or both, to ensure better clinical outcomes in patients with acute renal failure and end-stage renal disease, the use of continuous or long-term treatment with an artificial kidney is limited to less than 10% of patients with these diseases due to the requirement for hospitalization and the high financial costs (168). The majority of patients with these diseases must rely on traditional intermittent in-center dialysis, which greatly affects their quality of life and results in the periodic accumulation of metabolic wastes and toxins. A wearable or implantable artificial kidney, with a reasonable cost–effectiveness ratio, holds the promise not only of improving clinical outcomes in larger patient cohorts via its ability to perform daily or continuous dialysis, but also in allowing for a better quality of life by enabling home dialysis or even dialysis during travel. Different approaches have been used to develop miniaturized artificial kidneys, and reviews are available elsewhere (168, 169). It is noteworthy that artificial kidneys demand high-throughput processing that allows for input blood flows on the order of 100 mL/min, and many microfluidic artificial kidneys belong to the category of bioartificial kidneys, in which the biomimetic structure of renal tubule progenitor cells or epithelial cell culture is enabled by microelectromechanical system-based tissue engineering.

Figure 5

(*a*) Schematic of the circulating tumor cell (CTC) trap design. Up to 5 liters of blood from a patient is circulated through a functionalized membrane (i.e., coated with a cocktail of antibodies) for continuous large-scale CTC separation and analysis. The separated cells can be cultured ex vivo in Petri dishes for further characterization. Panel *a* adapted from Reference 151 with permission from the Multidisciplinary Digital Publishing Institute. (*b*, *i*) Schematic of a three-channel margination microdevice for separating bacteria from blood. (*b*, *ii*) Optical image of the prefiltration and bifurcation regions. (*b*, *iii*) Separation at each bifurcation. (*b*, *iv*) Schematic of the closed circuit used for coupling the device to a catheterized mouse using a peristaltic pump. Blood loss (approximately 30%) is compensated for by adding saline to the loop. Panel *b* adapted from Reference 167 with permission from the Royal Society of Chemistry. (*c*, *i*) Schematic of, and working principle for, a spiral microfluidic device with multiple outlets for continuous cell synchronization. Under the influence of inertial lift and Dean drag forces, asynchronous cell populations are fractionated by size to obtain relatively pure populations of cells in the G_0/G_1, S, and G_2/M phases. The cells in the G_2/M phase, due to their larger diameter, equilibrate near the inner wall of the microchannel; cells in the S and the G_0/G_1 phases then exit the device from outlets 1, 2, and 3, respectively. (*c*, *ii*) Distribution of DNA content of sorted human mesenchymal stem cells postsynchronization using a spiral device. Panel *c* adapted from Reference 186 with permission from the Royal Society of Chemistry.

3.5. Cleansing Banked Blood for Allogeneic Transfusion

Annually, more than 16 million units of stored blood are required for transfusion medicine in the United States, which places a massive burden on blood banks (170). Allogeneic transfusion of packed RBCs is the primary method for replenishing blood lost during surgery (171). Careful control of the quality of stored blood is tremendously important to ensuring positive clinical outcomes during allogeneic transfusion because the multitude of biochemical and physical changes occurring in RBCs during ex vivo storage (termed RBC storage lesions) can have lethal clinical consequences (172, 173). During the course of storage, the shape and function of RBCs can change significantly, causing serious problems during circulation after transfusion, such as occlusions in the microcirculation and, eventually, organ failure (101). Generally RBCs can be stored for up to 6 weeks, according to the United States Food and Drug Administration (174, 175). Sorting RBCs prior to transfusion could help ensure the quality of transfused blood and mitigate issues of interdonor heterogeneity by separating functioning, healthier (or good) RBCs from damaged (or bad) RBCs and their breakdown products. Microfluidic cell-sorting approaches could be particularly valuable for this purpose, given their portability and the ease of integrating them with existing blood-transfusion systems. An ideal RBC sorter should have throughput of approximately 100–175 mL/h, which is equivalent to the usual blood transfusion rate of approximately 2–3 h per unit of packed RBCs (i.e., 300–350 mL).

Recently, a few microfluidic systems have been developed to ensure safer blood transfusions. A team led by S. Shevkoplyas is currently working on a multiplexed microfluidic system for this purpose (176). Based on their online news report, it seems that they propose to mix packed RBCs with saline before passing them through a series of interconnected microchannels, which could separate good RBCs from bad, based on cell shape, size, and deformability. Although the details of this system have not been revealed, scaling microfluidic designs for processing larger volumes is reportedly a major hurdle. The Han group (177, 178) is investigating the applicability of using the μBM cell sorter to remove bad RBCs from refrigerated blood. Since the μBM device could separate deformable RBCs from their stiffer counterparts, the rationale for using the μBM device to improve blood transfusion lies in the fact that RBC aging and damage occurring during ex vivo storage coincide with a decrease in cellular deformability (179, 180). Through an in vitro study, Huang et al. (177) examined the evolution of the distribution of heterogeneous deformability in individual RBCs over storage time, and confirmed the association of RBC deformability with many clinical features that are important for posttransfusion clearance of RBCs. Specifically, when compared with deformable RBCs, the stiffer RBCs isolated by the μBM device displayed higher mechanical retention in the spleen, deteriorated osmotic fragility, and higher microparticle content. These results are in agreement with previous findings (174, 178, 181) and support the use of single RBC deformability as a biomarker to separate good RBCs from bad. Additionally, this margination system has already been tested for higher throughput (approximately 150 mL/h) using whole blood (167), making it a good candidate for clinical applications.

3.6. Large-Scale Cell Synchronization

Cell synchronization is commonly performed in biology to collect cells that are at the same phase of the cell cycle to comprehensively study their cellular properties and the genetic mechanisms involved in the phase prior to division (182). The cell cycle comprises a series of sequential events, mainly the duplication of DNA (the S phase) and the formation of daughter cells (M phase), along with two intermittent gap phases (G_1 and G_2) (80). Currently, there are two distinct strategies for cell synchronization, namely a chemical approach (known as arrest and release), and physical

methods (using size, density, and affinity). In the chemical approach, specific chemicals are used in the culture media to arrest cells at a particular phase (e.g., by inhibiting DNA replication during the S phase by using hydroxyurea or methotrexate); they are then released in synchrony by using a second chemical agent (183). A major problem with chemical approaches is the undesirable effect of disturbing the normal physiology of the cells and causing serious damage to cell growth, as well as disrupting progression through the cell cycle (58). Another obstacle is the throughput of chemical approaches, which is usually not high enough for large-scale experiments.

However, physical methods have been reported to cause negligible perturbation to the growth and progression of the synchronized cells. Of note, FACS and centrifugal elutriation (see Section 2.2.4) have been used widely in cell biology. Light scattering and the intensity of the fluorescent signal are two parameters routinely used in FACS for cell synchronization; however, the impaired viability of the synchronized cells as well as the associated costs are major hurdles that need to be overcome before large-scale operation is implemented. In centrifugal elutriation, differences in cell size and in the sedimentation density of living cells are exploited to fractionate cells during different phases of the cell cycle (80). Although FACS remains the gold standard in cell biology, and has extremely high throughput, it typically involves labor-intensive sample preparation and requires a large amount of space.

During the past decades, various microfluidic approaches have been proposed to achieve cell-cycle synchrony. Some methods, such as DEP (184) and hydrophoresis (185), have demonstrated good results and achieved high levels of synchrony; however, the insufficient throughput of these systems (approximately 10^4–10^5 cells/h) limits their real-world applications. Thévoz et al. (120) used acoustophoresis and reported higher throughputs for synchronization of mammalian cells (3×10^6 cells/h per microchannel). Using inertial microfluidics, Lee et al. (186) developed a high-throughput spiral biochip (**Figure 5*c***) that can efficiently fractionate several asynchronous mammalian cell lines, as well as mesenchymal stem cells, into enriched subpopulations with a throughput of around 15×10^6 cells/h. We are currently working on a multiplexed version of our biochip to be used in industrial applications; it has a throughput of approximately 10^7 cells/min, comparable to the yield of centrifugal elutriation systems or even hydrocyclones. This multiplexed system has distinct advantages over other cell-synchronization methods, including continuous operation and collection of cells. In addition, the passive nature of the inertial system eliminates the need for an externally applied field (e.g., an electrical or magnetic field) or even for direct modification of the cells via molecular labeling, thus further reducing processing time and costs.

4. CONCLUSIONS AND OUTLOOK

The creation of microfluidic particle-sorting systems has facilitated the analysis of small sample volumes at varying throughput rates. A myriad of microfluidic techniques has been developed, and reviews commonly classify them as affinity-based versus label-free, biochemical versus biophysical, or positive versus negative enrichment. In this review, we have focused primarily on the throughput of microfluidic particle-sorting methods, particularly those that can handle large sample volumes. We evaluated the strengths and weaknesses of each particle-sorting technique to provide a guide for choosing the appropriate technique for different applications. Our rationale for adopting this approach lies in our interest in capitalizing on the unique advantages provided by microfluidic cell handling to high-throughput applications, such as intraoperative blood salvage and extracorporeal blood purification for sepsis therapy, applications in which conventional bulk-scale processing methods suffer from limitations. Up until now, despite the superior purity and efficiency offered by microfluidic systems and the rapid growth in the literature about microfluidic particle-sorting techniques, commercial realization of these technologies remains low, and they

are mainly limited to point-of-care diagnostic use, partially due to the incompatibility of many microfluidic systems with large-volume sample-processing systems. The physics of fluid manipulation may be distinctively different at the macro- and microscales, but the successful creation of microscale counterflow elutriation devices and hydrocyclones demonstrates the possibility of combining the advantages of both macro- and microscale particle-sorting techniques. Additionally, the processes of parallelization and stacking can also boost the throughput of microfluidic techniques and enable the handling of large volumes of liquid to achieve biomedical objectives. We hope that this review offers a new perspective for assessing the suitability of microfluidic particle-sorting methods for objectives beyond low-volume sample processing.

DISCLOSURE STATEMENT

The authors are not aware of any affiliations, memberships, funding, or financial holdings that might be perceived as affecting the objectivity of this review.

ACKNOWLEDGMENTS

This research was supported by the National Research Foundation of Singapore through the Singapore–MIT Alliance for Research and Technology's BioSystems and Micromechanics Interdisciplinary Research Group program, as well as a grant from the US Advanced Research Projects Agency–Energy (grant number DE-AR0000294).

LITERATURE CITED

1. El-Ali J, Sorger PK, Jensen KF. 2006. Cells on chips. *Nature* 442(7101):403–11
2. Terry VH, Johnston ICD, Spina CA. 2009. CD44 MicroBeads accelerate HIV-1 infection in T cells. *Virology* 388(2):294–304
3. Takaishi S, Okumura T, Tu S, Wang SS, Shibata W, et al. 2009. Identification of gastric cancer stem cells using the cell surface marker CD44. *Stem Cells* 27(5):1006–20
4. Manz A, Graber N, Widmer HM. 1990. Miniaturized total chemical analysis systems: a novel concept for chemical sensing. *Sens. Actuators B: Chem.* 1(1–6):244–48
5. Weinberg E, Kaazempur-Mofrad M, Borenstein J. 2008. Concept and computational design for a bioartificial nephron-on-a-chip. *Int. J. Artif. Organs* 31(6):508–14
6. Hou HW, Bhagat AAS, Lee WC, Huang S, Han J, Lim CT. 2011. Microfluidic devices for blood fractionation. *Micromachines* 2(3):319–43
7. Martel JM, Toner M. 2014. Inertial focusing in microfluidics. *Annu. Rev. Biomed. Eng.* 16:371–96
8. Toner M, Irimia D. 2005. Blood-on-a-chip. *Annu. Rev. Biomed. Eng.* 7:77–103
9. Gossett DR, Weaver WM, Mach AJ, Hur SC, Tse HT, et al. 2010. Label-free cell separation and sorting in microfluidic systems. *Anal. Bioanal. Chem.* 397(8):3249–67
10. Bhagat AAS, Bow H, Hou HW, Tan SJ, Han J, Lim CT. 2010. Microfluidics for cell separation. *Med. Biol. Eng. Comput.* 48(10):999–1014
11. Pamme N. 2007. Continuous flow separations in microfluidic devices. *Lab Chip* 7(12):1644–59
12. Warkiani ME, Lou C-P, Gong H-Q. 2011. Fabrication of multi-layer polymeric micro-sieve having narrow slot pores with conventional ultraviolet-lithography and micro-fabrication techniques. *Biomicrofluidics* 5(3):036504
13. Chen L, Warkiani ME, Liu H-B, Gong H-Q. 2010. Polymeric micro-filter manufactured by a dissolving mold technique. *J. Micromech. Microeng.* 20(7):075005
14. Tan SJ, Yobas L, Lee GY, Ong CN, Lim CT. 2009. Microdevice for the isolation and enumeration of cancer cells from blood. *Biomed. Microdevices* 11(4):883–92
15. Wilding P, Kricka LJ, Cheng J, Hvichia G, Shoffner MA, Fortina P. 1998. Integrated cell isolation and polymerase chain reaction analysis using silicon microfilter chambers. *Anal. Biochem.* 257(2):95–100

16. Chung J, Shao H, Reiner T, Issadore D, Weissleder R, Lee H. 2012. Microfluidic cell sorter (μFCS) for on-chip capture and analysis of single cells. *Adv. Healthcare Mater.* 1(4):432–36
17. Liu Z, Huang F, Du J, Shu W, Feng H, et al. 2013. Rapid isolation of cancer cells using microfluidic deterministic lateral displacement structure. *Biomicrofluidics* 7(1):011801
18. Chabert M, Viovy J-L. 2008. Microfluidic high-throughput encapsulation and hydrodynamic self-sorting of single cells. *PNAS* 105(9):3191–96
19. Mach AJ, Di Carlo D. 2010. Continuous scalable blood filtration device using inertial microfluidics. *Biotechnol. Bioeng.* 107(2):302–11
20. Warkiani ME, Guan G, Luan KB, Lee WC, Bhagat AAS, et al. 2014. Slanted spiral microfluidics for the ultra-fast, label-free isolation of circulating tumor cells. *Lab Chip* 14(1):128–37
21. Bhardwaj P, Bagdi P, Sen A. 2011. Microfluidic device based on a micro-hydrocyclone for particle–liquid separation. *Lab Chip* 11(23):4012–21
22. Hoshino K, Huang YY, Lane N, Huebschman M, Uhr JW, et al. 2011. Microchip-based immunomagnetic detection of circulating tumor cells. *Lab Chip* 11(20):3449–57
23. Petersson F, Nilsson A, Holm C, Jonsson H, Laurell T. 2004. Separation of lipids from blood utilizing ultrasonic standing waves in microfluidic channels. *Analyst* 129(10):938–43
24. Hou HW, Bhagat AA, Chong AG, Mao P, Tan KS, et al. 2010. Deformability based cell margination—a simple microfluidic design for malaria-infected erythrocyte separation. *Lab Chip* 10(19):2605–13
25. Karabacak NM, Spuhler PS, Fachin F, Lim EJ, Pai V et al. 2014. Microfluidic, marker-free isolation of circulating tumor cells from blood samples. *Nat. Protoc.* 9(3):694–710
26. Mohamed H, Murray M, Turner JN, Caggana M. 2009. Isolation of tumor cells using size and deformation. *J. Chromatogr. A* 1216(47):8289–95
27. Lee D, Sukumar P, Mahyuddin A, Choolani M, Xu G. 2010. Separation of model mixtures of ε-globin positive fetal nucleated red blood cells and anucleate erythrocytes using a microfluidic device. *J. Chromatogr. A* 1217(11):1862–66
28. Murthy SK, Sethu P, Vunjak-Novakovic G, Toner M, Radisic M. 2006. Size-based microfluidic enrichment of neonatal rat cardiac cell populations. *Biomed. Microdevices* 8(3):231–37
29. Warkiani ME, Lou CP, Liu HB, Gong HQ. 2012. A high-flux isopore micro-fabricated membrane for effective concentration and recovering of waterborne pathogens. *Biomed. Microdevices* 14(4):669–77
30. Warkiani ME, Chen L, Lou C-P, Liu H-B, Zhang R, Gong H-Q. 2011. Capturing and recovering of *Cryptosporidium parvum* oocysts with polymeric micro-fabricated filter. *J. Membr. Sci.* 369(1):560–68
31. Aran K, Morales M, Sasso LA, Lo J, Zheng M, et al. 2011. Microfiltration device for continuous, label-free bacteria separation from whole blood for sepsis treatment. In *15th International Conference on Miniaturized Systems for Chemistry and Life Sciences* (*MicroTAS 2011*), ed. J Landers, pp. 497–500. San Diego, CA: Chemical and Biological Microsystems Society
32. Li X, Chen W, Liu G, Lu W, Fu J. 2014. Continuous-flow microfluidic blood cell sorting for unprocessed whole blood using surface-micromachined microfiltration membranes. *Lab Chip* 14(14):2565–75
33. Chen W, Huang NT, Oh B, Lam RH, Fan R, et al. 2013. Surface-micromachined microfiltration membranes for efficient isolation and functional immunophenotyping of subpopulations of immune cells. *Adv. Healthc. Mater.* 2(7):965–75
34. Warkiani ME, Bhagat AAS, Khoo BL, Han J, Lim CT, et al. 2013. Isoporous micro/nanoengineered membranes. *ACS Nano* 7(3):1882–904
35. Huang LR, Cox EC, Austin RH, Sturm JC. 2004. Continuous particle separation through deterministic lateral displacement. *Science* 304(5673):987–90
36. Inglis DW, Davis JA, Austin RH, Sturm JC. 2006. Critical particle size for fractionation by deterministic lateral displacement. *Lab Chip* 6(5):655–58
37. Davis JA, Inglis DW, Morton KJ, Lawrence DA, Huang LR, et al. 2006. Deterministic hydrodynamics: taking blood apart. *PNAS* 103(40):14779–84
38. Inglis DW, Herman N, Vesey G. 2010. Highly accurate deterministic lateral displacement device and its application to purification of fungal spores. *Biomicrofluidics* 4(2):024109
39. Huang R, Barber TA, Schmidt MA, Tompkins RG, Toner M, et al. 2008. A microfluidics approach for the isolation of nucleated red blood cells (NRBCs) from the peripheral blood of pregnant women. *Prenat. Diagn.* 28(10):892–99

40. Inglis DW, Lord M, Nordon RE. 2011. Scaling deterministic lateral displacement arrays for high throughput and dilution-free enrichment of leukocytes. *J. Micromech. Microeng.* 21(5):054024
41. Li N, Kamei DT, Ho CM. 2007. On-chip continuous blood cell subtype separation by deterministic lateral displacement. In *Nano/Micro Engineered and Molecular Systems*, pp. 932–36. New York: IEEE (Inst. Electr. Electron. Eng.)
42. Bowman TJ, Drazer G, Frechette J. 2013. Inertia and scaling in deterministic lateral displacement. *Biomicrofluidics* 7(6):64111
43. Inglis DW. 2009. Efficient microfluidic particle separation arrays. *Appl. Phys. Lett.* 94(1):013510
44. Loutherback K, Chou KS, Newman J, Puchalla J, Austin RH, et al. 2010. Improved performance of deterministic lateral displacement arrays with triangular posts. *Microfluid. Nanofluid.* 9(6):1143–49
45. Loutherback K, D'Silva J, Liu L, Wu A, Austin RH, Sturm JC. 2012. Deterministic separation of cancer cells from blood at 10 mL/min. *AIP Adv.* 2(4):042107
46. Zhou J, Papautsky I. 2013. Fundamentals of inertial focusing in microchannels. *Lab Chip* 13(6):1121–32
47. Yamada M, Nakashima M, Seki M. 2004. Pinched flow fractionation: continuous size separation of particles utilizing a laminar flow profile in a pinched microchannel. *Anal. Chem.* 76(18):5465–71
48. Takagi J, Yamada M, Yasuda M, Seki M. 2005. Continuous particle separation in a microchannel having asymmetrically arranged multiple branches. *Lab Chip* 5(7):778–84
49. Yamada M, Seki M. 2005. Hydrodynamic filtration for on-chip particle concentration and classification utilizing microfluidics. *Lab Chip* 5(11):1233–39
50. Tsutsui H, Ho C-M. 2009. Cell separation by non-inertial force fields in microfluidic systems. *Mech. Res. Commun.* 36(1):92–103
51. Kersaudy-Kerhoas M, Dhariwal R, Desmulliez MPY, Jouvet L. 2010. Hydrodynamic blood plasma separation in microfluidic channels. *Microfluid. Nanofluid.* 8(1):105–14
52. Di Carlo D. 2009. Inertial microfluidics. *Lab Chip* 9(21):3038–46
53. Di Carlo D, Irimia D, Tompkins RG, Toner M. 2007. Continuous inertial focusing, ordering, and separation of particles in microchannels. *PNAS* 104(48):18892–97
54. Ookawara S, Irimia D, Tompkins RG, Toner M. 2007. Quasi-direct numerical simulation of lift force-induced particle separation in a curved microchannel by use of a macroscopic particle model. *Chem. Eng. Sci.* 62(9):2454–65
55. Amini H, Lee W, Di Carlo D. 2014. Inertial microfluidic physics. *Lab Chip* 14(15):2739–61
56. Kuntaegowdanahalli SS, Bhagat AA, Kumar G, Papautsky I. 2009. Inertial microfluidics for continuous particle separation in spiral microchannels. *Lab Chip* 9(20):2973–80
57. Chatterjee A, Kuntaegowdanahalli SS, Papautsky I. 2011. Inertial microfluidics for continuous separation of cells and particles. *Proc. SPIE* 7929:792907
58. Lee W, Bhagat A, Lim C. 2014. High-throughput synchronization of mammalian cell cultures by spiral microfluidics. In *Animal Cell Biotechnology: Methods and Protocols*, ed. R Pörtner, pp. 3–13. New York: Humana. 3rd ed.
59. Wu L, Guan G, Hou HW, Bhagat AAS, Han J. 2012. Separation of leukocytes from blood using spiral channel with trapezoid cross-section. *Anal. Chem.* 84(21):9324–31
60. Guan G, Wu L, Bhagat AA, Li Z, Chen PC, Chao S, et al. 2013. Spiral microchannel with rectangular and trapezoidal cross-sections for size based particle separation. *Sci. Rep.* 3:1475
61. Bhagat AAS, Hou HW, Li LD, Lim CT, Han J. 2011. Pinched flow coupled shear-modulated inertial microfluidics for high-throughput rare blood cell separation. *Lab Chip* 11(11):1870–78
62. Wu Z, Willing B, Bjerketorp J, Jansson JK, Hjort K. 2009. Soft inertial microfluidics for high throughput separation of bacteria from human blood cells. *Lab Chip* 9(9):1193–99
63. Hou HW, Warkiani ME, Khoo BL, Li ZR, Soo RA, et al. 2013. Isolation and retrieval of circulating tumor cells using centrifugal forces. *Sci. Rep.* 3:1259
64. Warkiani ME, Khoo BL, Tan DS-W, Bhagat AAS, Lim W-T, et al. 2014. An ultra-high-throughput spiral microfluidic biochip for the enrichment of circulating tumor cells. *Analyst* 139(13):3245–55
65. Khoo BL, Warkiani ME, Tan DS, Bhagat AA, Irwin D, et al. 2014. Clinical validation of an ultra high-throughput spiral microfluidics for the detection and enrichment of viable circulating tumor cells. *PLOS ONE* 9(7):e99409

66. Hur SC, Henderson-MacLennan NK, McCabe ERB, Di Carlo D. 2011. Deformability-based cell classification and enrichment using inertial microfluidics. *Lab Chip* 11(5):912–20
67. Zheng S, Lin HK, Lu B, Williams A, Datar R, et al. 2011. 3D microfilter device for viable circulating tumor cell (CTC) enrichment from blood. *Biomed. Microdevices* 13(1):203–13
68. Xuan X, Zhu J, Church C. 2010. Particle focusing in microfluidic devices. *Microfluid. Nanofluid.* 9(1):1–16
69. Seo J, Lean MH, Kole A. 2007. Membraneless microseparation by asymmetry in curvilinear laminar flows. *J. Chromatogr. A* 1162(2):126–31
70. Vieira L, Barbosa Z, Damasceno JJR, Barrozo MAS. 2005. Performance analysis and design of filtering hydrocyclones. *Braz. J. Chem. Eng.* 22(1):143–52
71. Hwang K-J, Hsueh W-S, Nagase Y. 2008. Mechanism of particle separation in small hydrocyclone. *Dry. Technol.* 26(8):1002–10
72. Pinto RC, Medronho RA, Castilho LR. 2008. Separation of CHO cells using hydrocyclones. *Cytotechnology* 56(1):57–67
73. Habibian M, Pazouki M, Ghanaie H, Abbaspour-Sani K. 2008. Application of hydrocyclone for removal of yeasts from alcohol fermentations broth. *Chem. Eng. J.* 138(1):30–34
74. Bagdi P, Sen A, Bhardwaj P. 2012. Analysis and simulation of a micro hydrocyclone device for particle liquid separation. *J. Fluids Eng.* 134(2):021105
75. Hwang K-J, Hwang Y-W, Yoshida H. 2013. Design of novel hydrocyclone for improving fine particle separation using computational fluid dynamics. *Chem. Eng. Sci.* 85:62–68
76. Morijiri T, Hikida T, Yamada M, Seki M. 2011. Microfluidic counterflow centrifugal elutriation for cell separation using density-gradient media. In *14th International Conference on Miniaturized Systems for Chemistry and Life Sciences* (*MicroTAS 2010*), ed. S Verpoorte, pp. 722–24. San Diego, CA: Chemical and Biological Microsystems Society
77. Lindahl PE. 1948. Principle of a counter-streaming centrifuge for the separation of particles of different sizes. *Nature* 161:648–49
78. Grabske RJ, Lake S, Gledhill BL, Meistrich ML. 1975. Centrifugal elutriation: separation of spermatogenic cells on the basis of sedimentation velocity. *J. Cell. Physiol.* 86(1):177–89
79. Grosse J, Meier K, Bauer TJ, Eilles C, Grimm D. 2012. Cell separation by countercurrent centrifugal elutriation: recent developments. *Prep. Biochem. Biotechnol.* 42(3):217–33
80. Banfalvi G. 2008. Cell cycle synchronization of animal cells and nuclei by centrifugal elutriation. *Nat. Protoc.* 3(4):663–73
81. Morijiri T, Yamada M, Hikida T, Seki M, et al. 2013. Microfluidic counterflow centrifugal elutriation system for sedimentation-based cell separation. *Microfluid. Nanofluid.* 14(6):1049–57
82. Jandt U, Platas Barradas O, Pörtner R, Zeng AP. 2014. Mammalian cell culture synchronization under physiological conditions and population dynamic simulation. *Appl. Microbiol. Biotechnol.* 98(10):4311–19
83. Gorantla S, Che M, Gendelman HE. 2014. Centrifugal elutriation for studies of neuroimmunity. In *Current Laboratory Methods in Neuroscience Research*, ed. H Xiong, HE Gendelman, pp. 165–75. New York: Springer
84. Burger R, Kirby D, Glynn M, Nwankire C, O'Sullivan M, et al. 2012. Centrifugal microfluidics for cell analysis. *Curr. Opin. Chem. Biol.* 16(3):409–14
85. Ducrée J, Haeberle S, Lutz S, Pausch S, von Stetten F, Zengerle R. 2007. The centrifugal microfluidic bio-disk platform. *J. Micromech. Microeng.* 17(7):S103
86. Haeberle S, Brenner T, Zengerle R, Ducrée J. 2006. Centrifugal extraction of plasma from whole blood on a rotating disk. *Lab Chip* 6(6):776–81
87. Zhang J, Guo Q, Liu M, Yang J. 2008. A lab-on-CD prototype for high-speed blood separation. *J. Micromech. Microeng.* 18(12):125025
88. Li T, Zhang L, Leung KM, Yang J. 2010. Out-of-plane microvalves for whole blood separation on lab-on-a-CD. *J. Micromech. Microeng.* 20(10):105024
89. Shiono H, Ito Y. 2003. Novel method for continuous cell separation by density gradient centrifugation: evaluation of a miniature separation column. *Prep. Biochem. Biotechnol.* 33(2):87–100
90. Shiono H, Okada T, Ito Y. 2005. Application of a novel continuous-flow cell separation method for separation of cultured human mast cells. *J. Liquid Chromatogr. Relat. Technol.* 28(12–13):2071–83

91. Shiono H, Chen HM, Okada T, Ito Y. 2007. Colony-forming cell assay for human hematopoietic progenitor cells harvested by a novel continuous-flow cell separation method. *J. Chromatogr. A* 1151(1–2):153–57
92. Martinez-Duarte R, Gorkin RA 3rd, Abi-Samra K, Madou MJ. 2010. The integration of 3D carbon-electrode dielectrophoresis on a CD-like centrifugal microfluidic platform. *Lab Chip* 10(8):1030–43
93. Madou M, Zoval J, Jia G, Kido H, Kim J, Kim N. 2006. Lab on a CD. *Annu. Rev. Biomed. Eng.* 8:601–28
94. Gorkin R, Park J, Siegrist J, Amasia M, Lee BS, et al. 2010. Centrifugal microfluidics for biomedical applications. *Lab Chip* 10(14):1758–73
95. Amasia M, Siegrist J, Madou M. 2011. Large-volume centrifugal microfluidic device for whole blood sample preparation. In *14th International Conference on Miniaturized Systems for Chemistry and Life Sciences 2010* (*MicroTAS 2010*), ed. S Verpoorte, pp. 815–17. San Diego, CA: Chemical and Biological Microsystems Society
96. Picot J, Guerin CL, Le Van Kim C, Boulanger CM. 2012. Flow cytometry: retrospective, fundamentals and recent instrumentation. *Cytotechnology* 64(2):109–30
97. Kiermer V. 2005. FACS-on-a-chip. *Nat. Methods* 2(2):91
98. Johansson L, Nikolajeff F, Johansson S, Thorslund S. 2009. On-chip fluorescence-activated cell sorting by an integrated miniaturized ultrasonic transducer. *Anal. Chem.* 81(13):5188–96
99. Lenshof A, Laurell T. 2010. Continuous separation of cells and particles in microfluidic systems. *Chem. Soc. Rev.* 39(3):1203–17
100. Gao Y, Li W, Pappas D. 2013. Recent advances in microfluidic cell separations. *Analyst* 138(17):4714–21
101. Collins TA. 2011. Packed red blood cell transfusions in critically ill patients. *Crit. Care Nurse* 31(1):25–34
102. Kang JH, Krause S, Tobin H, Mammoto A, Kanapathipillai M, Ingber DE. 2012. A combined micromagnetic-microfluidic device for rapid capture and culture of rare circulating tumor cells. *Lab Chip* 12(12):2175–81
103. Yung CW, Fiering J, Mueller AJ, Ingber DE. 2009. Micromagnetic–microfluidic blood cleansing device. *Lab Chip* 9(9):1171–77
104. Gorges T, Tinhofer I, Drosch M, Röse L, Zollner TM, et al. 2012. Circulating tumour cells escape from EpCAM-based detection due to epithelial-to-mesenchymal transition. *BMC Cancer* 12(1):1–13
105. Liu Z, Fusi A, Klopocki E, Schmittel A, Tinhofer I, et al. 2011. Negative enrichment by immunomagnetic nanobeads for unbiased characterization of circulating tumor cells from peripheral blood of cancer patients. *J. Transl. Med.* 9(1):70
106. Naume B, Borgen E, Nesland JM, Beiske K, Gilen E, et al. 1998. Increased sensitivity for detection of micrometastases in bone-marrow/peripheral-blood stem-cell products from breast-cancer patients by negative immunomagnetic separation. *Int. J. Cancer* 78(5):556–60
107. Chen C-L, Chen KC, Pan YC, Lee TP, Hsiung LC, et al. 2011. Separation and detection of rare cells in a microfluidic disk via negative selection. *Lab Chip* 11(3):474–83
108. Dainiak MB, Galaev IY, Kumar A, Plieva FM, Mattiasson B. 2007. Chromatography of living cells using supermacroporous hydrogels, *cryogels*. *Adv. Biochem. Eng. Biotechnol.* 106:101–27
109. Plieva FM, Galaev IY, Noppe W, Mattiasson B. 2008. Cryogel applications in microbiology. *Trends Microbiol.* 16(11):543–51
110. Kumar A, Bhardwaj A. 2008. Methods in cell separation for biomedical application: cryogels as a new tool. *Biomed. Mater.* 3(3):034008
111. Wang Z, Zhe J. 2011. Recent advances in particle and droplet manipulation for lab-on-a-chip devices based on surface acoustic waves. *Lab Chip* 11(7):1280–85
112. Shi J, Huang H, Stratton Z, Huang Y, Huang TJ. 2009. Continuous particle separation in a microfluidic channel via standing surface acoustic waves (SSAW). *Lab Chip* 9(23):3354–59
113. Wiklund M, Hertz HM. 2006. Ultrasonic enhancement of bead-based bioaffinity assays. *Lab Chip* 6(10):1279–92
114. Laurell T, Petersson F, Nilsson A. 2007. Chip integrated strategies for acoustic separation and manipulation of cells and particles. *Chem. Soc. Rev.* 36(3):492–506
115. Lenshof A, Laurell T. 2011. Emerging clinical applications of microchip-based acoustophoresis. *J. Assoc. Lab. Autom.* 16(6):443–49

116. Petersson F, Åberg L, Swärd-Nilsson A-M, Laurell T. 2007. Free flow acoustophoresis: microfluidic-based mode of particle and cell separation. *Anal. Chem.* 79(14):5117–23
117. Persson J, Augustsson P, Laurell T, Ohlin M. 2008. Acoustic microfluidic chip technology to facilitate automation of phage display selection. *FEBS J.* 275(22):5657–66
118. Lenshof A, Ahmad-Tajudin A, Järås K, Swärd-Nilsson A-M, Åberg L, et al. 2009. Acoustic whole blood plasmapheresis chip for prostate specific antigen microarray diagnostics. *Anal. Chem.* 81(15):6030–37
119. Dykes J, Lenshof A, Åstrand-Grundström I-B, Laurell T, Scheding S. 2011. Efficient removal of platelets from peripheral blood progenitor cell products using a novel micro-chip based acoustophoretic platform. *PLOS ONE* 6(8):e23074
120. Thévoz P, Adams JD, Shea H, Bruus H, Soh HT. 2010. Acoustophoretic synchronization of mammalian cells in microchannels. *Anal. Chem.* 82(7):3094–98
121. Augustsson P, Magnusson C, Nordin M, Lilja H, Laurell T. 2012. Microfluidic, label-free enrichment of prostate cancer cells in blood based on acoustophoresis. *Anal. Chem.* 84(18):7954–62
122. Yang AH, Soh HT. 2012. Acoustophoretic sorting of viable mammalian cells in a microfluidic device. *Anal. Chem.* 84(24):10756–62
123. Shi J, Mao X, Ahmed D, Colletti A, Huang TJ. 2008. Focusing microparticles in a microfluidic channel with standing surface acoustic waves (SSAW). *Lab Chip* 8(2):221–23
124. Grenvall C, Augustsson P, Folkenberg JR, Laurell T. 2009. Harmonic microchip acoustophoresis: a route to online raw milk sample precondition in protein and lipid content quality control. *Anal. Chem.* 81(15):6195–200
125. Trampler F, Sonderhoff SA, Pui PW, Kilburn DG, Piret JM. 1994. Acoustic cell filter for high density perfusion culture of hybridoma cells. *Nat. Biotechnol.* 12(3):281–84
126. Hammarstrom B, Laurell T, Nilsson J. 2012. Seed particle-enabled acoustic trapping of bacteria and nanoparticles in continuous flow systems. *Lab Chip* 12(21):4296–304
127. Dung Luong T, Trung Nguyen N. 2010. Surface acoustic wave driven microfluidics—a review. *Micro Nanosyst.* 2(3):217–25
128. Long DS, Smith ML, Pries AR, Ley K, Damiano ER. 2004. Microviscometry reveals reduced blood viscosity and altered shear rate and shear stress profiles in microvessels after hemodilution. *PNAS* 101(27):10060–65
129. Geng Z, Zhang L, Ju Y, Wang W, Li Z. 2011. A plasma separation device based on centrifugal effect and Zweifach-Fung effect. In *15th International Conference on Miniaturized Systems for Chemistry and Life Sciences* (*MicroTAS 2011*), ed. J Landers, pp. 224–26. San Diego, CA: Chemical and Biological Microsystems Society
130. Jäggi R, Sandoz R, Effenhauser C. 2007. Microfluidic depletion of red blood cells from whole blood in high-aspect-ratio microchannels. *Microfluid. Nanofluid.* 3(1):47–53
131. Yang S, Undar A, Zahn JD. 2006. A microfluidic device for continuous, real time blood plasma separation. *Lab Chip* 6(7):871–80
132. Faivre M, Abkarian M, Bickraj K, Stone HA. 2006. Geometrical focusing of cells in a microfluidic device: an approach to separate blood plasma. *Biorheology* 43(2):147–59
133. Sollier E, Rostaing H, Pouteau P, Fouillet Y, Achard J-L. 2009. Passive microfluidic devices for plasma extraction from whole human blood. *Sens. Actuators B: Chem.* 141(2):617–24
134. Shevkoplyas SS, Yoshida T, Munn LL, Bitensky MW. 2005. Biomimetic autoseparation of leukocytes from whole blood in a microfluidic device. *Anal. Chem.* 77(3):933–37
135. Wei Hou H, Gan HY, Bhagat AA, Li LD, Lim CT, Han J. 2012. A microfluidics approach towards high-throughput pathogen removal from blood using margination. *Biomicrofluidics* 6(2):024115
136. Hur SC, Mach AJ, Di Carlo D. 2011. High-throughput size-based rare cell enrichment using microscale vortices. *Biomicrofluidics* 5(2):022206
137. Moon HS, Kwon K, Kim SI, Han H, Sohn J, et al. 2011. Continuous separation of breast cancer cells from blood samples using multi-orifice flow fractionation (MOFF) and dielectrophoresis (DEP). *Lab Chip* 11(6):1118–25
138. Sollier E, Go DE, Che J, Gossett DR, O'Byrne S, et al. 2014. Size-selective collection of circulating tumor cells using vortex technology. *Lab Chip* 14(1):63–77

139. Wang X, Zhou J, Papautsky I. 2013. Vortex-aided inertial microfluidic device for continuous particle separation with high size-selectivity, efficiency, and purity. *Biomicrofluidics* 7(4):044119
140. Song S, Choi S. 2014. Inertial modulation of hydrophoretic cell sorting and focusing. *Appl. Phys. Lett.* 104(7):074106
141. Adams JD, Thévoz P, Bruus H, Soh HT. 2009. Integrated acoustic and magnetic separation in microfluidic channels. *Appl. Phys. Lett.* 95(25):254103
142. Liu Z, Zhang W, Huang F, Feng H, Shu W, et al. 2013. High throughput capture of circulating tumor cells using an integrated microfluidic system. *Biosens. Bioelectron.* 47:113–19
143. Seo H, Kim H, Kim Y. 2011. Hydrodynamics and magnetophoresis based hybrid blood cell sorter for high throughput separation. In *14th International Conference on Miniaturized Systems for Chemistry and Life Sciences* (*MicroTAS 2010*), ed. S Verpoorte, pp. 223–25. San Diego, CA: Chemical and Biological Microsystems Society
144. Ozkumur E, Shah AM, Ciciliano JC, Emmink BL, Miyamoto DT, et al. 2013. Inertial focusing for tumor antigen–dependent and –independent sorting of rare circulating tumor cells. *Sci. Transl. Med.* 5(179):179ra47
145. Dharmasiri U, Witek MA, Adams AA, Soper SA. 2010. Microsystems for the capture of low-abundance cells. *Annu. Rev. Anal. Chem.* 3:409–31
146. Sleijfer S, Gratama JW, Sieuwerts AM, Kraan J, Martens JW, Foekens JA. 2007. Circulating tumour cell detection on its way to routine diagnostic implementation? *Eur. J. Cancer* 43(18):2645–50
147. Yu M, Bardia A, Aceto N, Bersani F, Madden MW, et al. 2014. Ex vivo culture of circulating breast tumor cells for individualized testing of drug susceptibility. *Science* 345(6193):216–20
148. Saucedo-Zeni N, Mewes S, Niestroj R, Gasiorowski L, Murawa D, et al. 2012. A novel method for the in vivo isolation of circulating tumor cells from peripheral blood of cancer patients using a functionalized and structured medical wire. *Int. J. Oncol.* 41(4):1241–50
149. Eifler RL, Lind J, Falkenhagen D, Weber V, Fischer MB, Zeillinger R 2011. Enrichment of circulating tumor cells from a large blood volume using leukapheresis and elutriation: proof of concept. *Cytometry B: Clin. Cytometry* 80(2):100–11
150. Fischer JC, Niederacher D, Topp SA, Honisch E, Schumacher S, et al. 2013. Diagnostic leukapheresis enables reliable detection of circulating tumor cells of nonmetastatic cancer patients. *PNAS* 110(41):16580–85
151. Barradas A, Terstappen LW. 2013. Towards the biological understanding of CTC: capture technologies, definitions and potential to create metastasis. *Cancers* 5(4):1619–42
152. Williamson KR, Taswell F. 1991. Intraoperative blood salvage: a review. *Transfusion* 31(7):662–75
153. Heiss MM, Mempel W, Delanoff C, Jauch KW, Gabka C, et al. 1994. Blood transfusion-modulated tumor recurrence: first results of a randomized study of autologous versus allogeneic blood transfusion in colorectal cancer surgery. *J. Clin. Oncol.* 12(9):1859–67
154. Moore FA, Moore EE, Sauaia A. 1997. Blood transfusion: an independent risk factor for postinjury multiple organ failure. *Arch. Surg.* 132(6):620–25
155. Johnson JL, Moore EE, Kashuk JL, Banerjee A, Cothren CC, et al. 2010. Effect of blood products transfusion on the development of postinjury multiple organ failure. *Arch. Surg.* 145(10):973–77
156. Waters JH, Yazer M, Chen YF, Kloke J. 2012. Blood salvage and cancer surgery: a meta-analysis of available studies. *Transfusion* 52(10):2167–73
157. Futamura N, Nakanishi H, Hirose H, Nakamura S, Tatematsu M. 2005. The effect of storage on the survival of cancer cells in blood and efficient elimination of contaminating cancer cells by a leukocyte depletion filter. *Am. Surg.* 71(7):585–90
158. Gwak MS, Lee KW, Kim SY, Lee J, Joh JW, et al. 2005. Can a leukocyte depletion filter (LDF) reduce the risk of reintroduction of hepatocellular carcinoma cells? *Liver Transplant.* 11(3):331–35
159. Rimmele T, Kellum J. 2011. Clinical review: blood purification for sepsis. *Crit. Care* 15(1):205
160. Angus DC, Linde-Zwirble WT, Lidicker J, Clermont G, Carcillo J, Pinsky MR. 2001. Epidemiology of severe sepsis in the United States: analysis of incidence, outcome, and associated costs of care. *Crit. Care Med.* 29(7):1303–10
161. Rimmelé T, Kaynar AM, McLaughlin JN, Bishop JV, Fedorchak MV, et al. 2013. Leukocyte capture and modulation of cell-mediated immunity during human sepsis: an ex vivo study. *Crit. Care* 17(2):R59

162. Devroe E. 2014. *Capture and Concentration of Microbial Pathogens*. Boston, MA: Wyss Inst. Biol. Inspired Eng. Harv. Univ., retrieved June 2, 2014. **http://wyss.harvard.edu/viewpage/462/**
163. Rimmele T, Kaynar AM, McLaughlin JN, Bishop JV, Fedorchak MV, et al. 2013. Leukocyte capture and modulation of cell-mediated immunity during human sepsis: an ex vivo study. *Crit. Care* 17(2):R59
164. Ding F, Song JH, Jung JY, Lou L, Wang M, et al. 2011. A biomimetic membrane device that modulates the excessive inflammatory response to sepsis. *PLOS ONE* 6(4):e18584
165. Hou HW, Gan HY, Bhagat AAS, Li LD, Lim CT, Han J. 2012. A microfluidics approach towards high-throughput pathogen removal from blood using margination. *Biomicrofluidics* 6(2):024115
166. Pries AR, Secomb TW, Gaehtgens P. 1996. Biophysical aspects of blood flow in the microvasculature. *Cardiovasc. Res.* 32(4):654–67
167. Hou HW, Vera MP, Levy BD, Baron RM, Han J. 2014. Novel microfluidic "cell-based" blood dialysis platform for murine model of sepsis. In *17th International Conference on Miniaturized Systems for Chemistry and Life Sciences* (*MicroTAS 2013*), ed. R Zengerie, pp. 1845–47. San Diego, CA: Chemical and Biological Microsystems Society
168. Ronco C, Davenport A, Gura V. 2011. The future of the artificial kidney: moving towards wearable and miniaturized devices. *Nefrologia* 31(1):9–16
169. Humes HD, Buffington D, Westover AJ, Roy S, Fissell WH. 2014. The bioartificial kidney: current status and future promise. *Pediatr. Nephrol.* 29(3):343–51
170. Toner RW, Pizzi L, Leas B, Ballas SK, Quigley A, Goldfarb NI. 2011. Costs to hospitals of acquiring and processing blood in the US. *Appl. Health Econ. Health Policy* 9(1):29–37
171. Carson JL, Grossman BJ, Kleinman S, Tinmouth AT, Marques MB, et al. 2012. Red blood cell transfusion: a clinical practice guideline from the AABB. *Ann. Intern. Med.* 157(1):49–58
172. Kor DJ, Van Buskirk CM, Gajic O. 2009. Red blood cell storage lesion. *Bosnian J. Basic Med. Sci.* 9(Suppl. 1):S21–27
173. Pavenski K, Saidenberg E, Lavoie M, Tokessy M, Branch DR. 2012. Red blood cell storage lesions and related transfusion issues: a Canadian blood services research and development symposium. *Transfus. Med. Rev.* 26(1):68–84
174. Luten M, Roerdinkholder-Stoelwinder B, Schaap NP, de Grip WJ, Bos HJ, Bosman GJ. 2008. Survival of red blood cells after transfusion: a comparison between red cells concentrates of different storage periods. *Transfusion* 48(7):1478–85
175. Dumont LJ, AuBuchon JP. 2008. Evaluation of proposed FDA criteria for the evaluation of radiolabeled red cell recovery trials. *Transfusion* 48(6):1053–60 [Biomedical Excellence for Safer Transfusion (BEST) Collaborative]
176. Merkl L. 2014. *UH Biomedical Engineer Works to Make Blood Transfusions Safer: NIH-funded Technology for Separating Well-preserved Red Blood Cells from Potentially Harmful Materials*. Houston, TX: Univ. Houst., retrieved June 2, 2014. **http://www.uh.edu/news-events/stories/2014/April/042314Shevkoplyas.php**
177. Huang S, Hou HW, Kanias T, Sertorio JT, Chen H, et al. 2015. Towards microfluidic-based depletion of stiff and fragile human red cells that accumulate during blood storage. *Lab Chip* 15:448–58
178. Huang S, Amaladoss A, Liu M, Chen H, Zhang R, et al. 2014. In vivo splenic clearance corresponds with in vitro deformability of red blood cells from *Plasmodium yoelii* infected mice. *Infect. Immunity* 82(6):2532–41
179. Farges E, Grebe R, Baumann M. 2002. Viscoelastic and biochemical properties of erythrocytes during storage with SAG-M at + 4°C. *Clin. Hemorheol. Microcirc.* 27(1):1–11
180. Kim-Shapiro DB, Lee J, Gladwin MT. 2011. Storage lesion: role of red blood cell breakdown. *Transfusion* 51(4):844–51
181. Deplaine G, Safeukui I, Jeddi F, Lacoste F, Brousse V, et al. 2011. The sensing of poorly deformable red blood cells by the human spleen can be mimicked in vitro. *Blood* 117(8):e88–95
182. Fox MH. 2004. Methods for synchronizing mammalian cells. In *Methods in Molecular Biology*, vol. 241: *Cell Cycle Checkpoint Control Protocols*, ed. HB Lieberman, pp. 11–16. Totowa, NJ: Humana
183. Coquelle A, Mouhamad S, Pequignot MO, Braun T, Carvalho G, et al. 2006. Enrichment of non-synchronized cells in the G1, S and G2 phases of the cell cycle for the study of apoptosis. *Biochem. Pharmacol.* 72(11):1396–404

184. Kim U, Shu CW, Dane KY, Daugherty PS, Wang JY, Soh HT. 2007. Selection of mammalian cells based on their cell-cycle phase using dielectrophoresis. *PNAS* 104(52):20708–12
185. Choi S, Song S, Choi C, Park JK. 2009. Microfluidic self-sorting of mammalian cells to achieve cell cycle synchrony by hydrophoresis. *Anal. Chem.* 81(5):1964–68
186. Lee WC, Bhagat AA, Huang S, Van Vliet KJ, Han J, Lim CT. 2011. High-throughput cell cycle synchronization using inertial forces in spiral microchannels. *Lab Chip* 11(7):1359–67